Neuropsychopharmacology (2011) 36, 1073–1089

www.neuropsychopharmacology.org

Huperzine A Activates Wnt/β-Catenin Signaling and Enhances the Nonamyloidogenic Pathway in an Alzheimer Transgenic Mouse Model

Chun-Yan Wang[1,4], Wei Zheng[1,4], Tao Wang[1], Jing-Wei Xie[1], Si-Ling Wang[2], Bao-Lu Zhao[3], Wei-Ping Teng[1] and Zhan-You Wang*[,1]

[1]Key Laboratory of Medical Cell Biology of Ministry of Education, and Key Laboratory of Endocrine Diseases of Liaoning Province, China Medical University, Shenyang, China; [2]Department of Pharmaceutics, Shenyang Pharmaceutical University, Shenyang, China; [3]State Key Laboratory of Brain and Cognitive Sciences, Institute of Biophysics, Academia Sinica, Beijing, PR China

Huperzine A (HupA) is a reversible and selective inhibitor of acetylcholinesterase (AChE), and it has multiple targets when used for Alzheimer's disease (AD) therapy. In this study, we searched for new mechanisms by which HupA could activate Wnt signaling and reduce amyloidosis in AD brain. A nasal gel containing HupA was prepared. No obvious toxicity of intranasal administration of HupA was found in mice. HupA was administered intranasally to β-amyloid (Aβ) precursor protein and presenilin-1 double-transgenic mice for 4 months. We observed an increase in ADAM10 and a decrease in BACE1 and APP695 protein levels and, subsequently, a reduction in Aβ levels and Aβ burden were present in HupA-treated mouse brain, suggesting that HupA enhances the nonamyloidogenic APP cleavage pathway. Importantly, our results further showed that HupA inhibited GSK3α/β activity, and enhanced the β-catenin level in the transgenic mouse brain and in SH-SY5Y cells overexpressing Swedish mutation APP, suggesting that the neuroprotective effect of HupA is not related simply to its AChE inhibition and antioxidation, but also involves other mechanisms, including targeting of the Wnt/β-catenin signaling pathway in AD brain.
Neuropsychopharmacology (2011) **36,** 1073–1089; doi:10.1038/npp.2010.245; published online 2 February 2011

Keywords: Alzheimer's disease; APP/PS1 transgenic mouse; β-catenin; glycogen synthase kinase; huperzine A; Wnt signaling

INTRODUCTION

Alzheimer's disease (AD), which is increasing in prevalence, is a long-term condition that is expensive to treat and is now a major public health problem for aging populations around the world. Pathologically, AD is characterized by extracellular β-amyloid (Aβ) plaques, intracellular neurofibrillary tangles, and selective cholinergic neuronal loss in the brain regions involved in learning and memory. Clinically, cholinesterase inhibitors, such as donepezil, galantamine, rivastigmine, and huperzine A (HupA), which are believed to act by blocking acetylcholine degradation and increasing the function of the surviving cholinergic neurons, have been shown to have beneficial effects by improving general cognitive function and reducing behavioral disturbances (Wang *et al*, 2001; Ceravolo *et al*, 2004; Erkinjuntti *et al*, 2004; Sicras and Rejas-Gutierrez, 2004; van der Staay and Bouger, 2005; Alisky, 2006; Mori *et al*, 2006). Recently, the multiple targets of cholinesterase inhibitors used to treat AD have received increasing attention (Lahiri *et al*, 2004; Zhang and Tang, 2006; Zhang *et al*, 2008a; Akaike *et al*, 2010).

The canonical Wnt signaling pathway has an important role in neuronal development and maintenance of the nervous system (Patapoutian and Reichardt, 2000). Recent studies have shown that Wnt signaling is involved in neurodegenerative diseases, especially in acetylcholinesterase (AChE) and Aβ-mediated neurotoxicity (Inestrosa *et al*, 2000; Garrido *et al*, 2002; De Ferrari *et al*, 2003). First, AChE is present in neuritic plaques in the AD brain (Geula and Mesulam, 1995; Guillozet *et al*, 1997), and can enhance Aβ aggregation and plaque formation and may form AChE–Aβ complexes (Alvarez *et al*, 1997). *In vivo* Aβ intrahippocampal injection and *in vitro* hippocampal neuronal culture experiments have shown that the AChE–Aβ complexes induce neuronal death more dramatically than Aβ peptide

*Correspondence: Professor Z-Y Wang, Key Laboratory of Medical Cell Biology of Ministry of Education, and Key Laboratory of Endocrine Diseases of Liaoning Province, China Medical University, Shenyang 110001, China, Tel: +8 61 399 889 1892, Fax: +86 24 23256666 5305, E-mail: wangzy@mail.cmu.edu.cn
[4]These authors contributed equally to this work.
Received 14 August 2010; revised 11 December 2010; accepted 14 December 2010

alone (Alvarez *et al*, 1998; Munoz and Inestrosa, 1999; Reyes *et al*, 2004). Second, the levels of glycogen synthase kinase-3β (GSK3β) and β-catenin, the two key molecules in the Wnt signaling pathway (Willert and Nusse, 1998; Moon *et al*, 2002), are altered dramatically in the brain of AD model mice (Zhang *et al*, 1998; Pei *et al*, 1999), and treatment with AChE–Aβ complexes reduces the level of cytoplasmic β-catenin in cultured hippocampal neurons (Alvarez *et al*, 2004). Finally, treatments with a Wnt cascade activator (lithium) or antagonist (Frzb-1) can protect against Aβ-induced neuronal death (Alvarez *et al*, 1999; Inestrosa *et al*, 2004). Taken together, these studies demonstrate that AChE–Aβ-dependent neurotoxicity may result in a loss of neuroprotection of Wnt signaling components, and that activation of Wnt signaling may prevent cholinergic neuronal degeneration in AD. However, whether the neuroprotective effect of cholinesterase inhibitors is related to the action of Wnt/β-catenin has not been fully clarified.

HupA is a novel lycopodium alkaloid extracted from the Chinese folk medicine, *Huperzia serrata*. HupA has several beneficial effects for AD patients (Wang *et al*, 2006a) and, in China it is one of the most commonly prescribed drugs for many forms of dementia, including AD (Zhang *et al*, 2008b). Apart from its well-known inhibitory effect on AChE (Zhu and Giacobini, 1995; Cheng *et al*, 1996; Cheng and Tang, 1998), HupA is considered to have multiple neuroprotective effects including anti-inflammatory and antioxidant properties (Wang and Tang, 2007; Wang *et al*, 2008; Zhang *et al*, 2008a), stimulation of the release of soluble α-secretase-derived fragments of APP (sAPPα) (Zhang *et al*, 2004; Peng *et al*, 2006; Yan *et al*, 2007), protection against Aβ and glutamate-induced neurotoxicity, and regulation of nerve growth factor (Ved *et al*, 1997; Tang *et al*, 2005). Interestingly, recent studies have shown that intranasal administration of a nasal gel containing HupA is a suitable system for delivery of HupA to the brain and, hence, provides a potential strategy for chronic AD therapy (Yue *et al*, 2007). Compared with the intravenous and oral administration for chronic disease such as AD, intranasal drug delivery does not require complicated medical services. The drug is not affected by the absorption on the basis of digestive tract circumstances and does not undergo first pass effect of liver (Yagi *et al*, 2002; Tang *et al*, 2008). HupA is a lipophilic weak alkaloid with a molecular weight of 242.32. It has a good permeability and can be transferred into the central nervous system via the nasal route (Yue *et al*, 2007). However, the neuroprotective effects of nasal gel HupA on AD transgenic mouse brain have never been evaluated.

In this study, human β-amyloid precursor protein and presenilin-1 (APP/PS1) double-transgenic mice were used to evaluate the safety of intranasal administration of HupA. Nasal gel HupA treatment did not show significant toxic effects on mice. We further assessed the known effects of HupA and investigated the possibility of a new mechanism of HupA on AD therapy. Our *in vivo* experimental results indicate that HupA inhibits the activity of GSK3, and increases the level of β-catenin in APP/PS1 mouse brain. Furthermore, the effects of HupA on inhibition of GSK3 and activation of β-catenin were confirmed using human neuroblastoma SH-SY5Y cells stably transfected with Swedish mutation APP (APPsw) *in vitro*. The present data suggest that the neuroprotective effect of HupA is not only related to its AChE inhibition, but also involves other mechanisms, particularly targeting of the Wnt/β-catenin signaling pathway in AD brain.

MATERIALS AND METHODS

Animals

APP/PS1 (APPswe/PSEN1dE9) double-transgenic mice and wild-type C57BL/6 mice were originally obtained from the Jackson Laboratory (West Grove, PA). They were kept in cages in a controlled environment (22–25 °C, 50% humidity, 12-h light/dark cycle), fed a standard diet, and distilled water was available *ad libitum*. All efforts were made to minimize animal suffering and the number of animals used. The experimental procedures were carried out in accordance with the Chinese regulations involving animal protection and approved by the animal ethics committee of the China Medical University.

Preparation of Nasal Gel Containing HupA and Administration to APP/PS1 Mice

HupA was purchased from Tau Biotech (Shanghai, China). The drug was 98% pure as determined by HPLC. All other chemicals were purchased from commercial suppliers and were of reagent grade or better. Nasal gel containing HupA was prepared according to a protocol described previously with minor modifications (Yue *et al*, 2007). Briefly, 100 mg HupA was dissolved in 1 ml hydrochloric acid (0.1 M). Nasal gel (8.5 ml) was made by mixing 5% (w/v) mannitol, 0.18% (w/v) methyl parahydroxybenzoate, and 0.02% (w/v) propyl parahydroxy benzoate in deionized water, heating to 90 °C, and then cooling to 40 °C. Next, 0.25% (w/v) carbomer and 0.1% (w/v) hydroxypropyl methylcellulose were added to the mixture. Finally, HupA (1 ml) was mixed with nasal gel (8.5 ml) and the pH adjusted to 5.8 with trihydroxymethyl aminomethane, and then deionized water was added to give a final volume of 10 ml. This resulted in nasal gel HupA with a concentration of 10 mg/ml that was ready for use.

APP/PS1 transgenic mice at 6 months of age were randomly assigned to three groups ($n = 7$ in each group), a vehicle control group and two nasal gel HupA groups, and treated intranasally once a day for 4 months with nasal gel and nasal gel containing HupA, at doses of 167 and 500 μg/kg, respectively. The doses of HupA chosen for this study were based on a previous report showing that intranasal administration of HupA, at 167 and 500 μg/kg, produced a dose-dependent increase in the drug concentration in the CSF and blood (Yue *et al*, 2007). Briefly, mice were hand-restrained in a supine position. Nasal gel HupA was given into one nostril according to the body weight using a pipette tip attached to a 10 μl microsyringe. After treatment, mice were kept in supine position for 1 min to ensure that nasal gel was inhaled. This drug delivery process was repeated daily through the other nostril alternately (Marks *et al*, 2009). To evaluate the effect of nasal gel HupA on APP/PS1 mouse brain, mice at the age of 10 months were anaesthetized with sodium pentobarbital (50 mg/kg, i.p.) and killed by decapitation. The brains were removed

immediately and split into halves. The right hemisphere was placed in 4% paraformaldehyde and embedded in paraffin for immunohistochemistry analyses, and the left hemisphere was kept at −80 °C for biochemical, immunoblot, RT-PCR. or ELISA analysis.

Scanning Electron Microscopy

Male C57BL/6 mice at 6 months of age were treated with nasal gel and nasal gel containing HupA at doses of 167 and 500 μg/kg, respectively. A test solution was administered to one side of the nostril once a day for seven consecutive days. At 24 h after the last administration, mice were killed and the nasal septum mucosa was removed. The samples were fixed with 2.5% glutaraldehyde solution followed by 1% osmic acid. After being dried at the critical point of carbon dioxide after dehydration, and coated with gold using an ion coater, the samples were examined and images were obtained using a scanning electron microscope (JSM-T300).

Nissl Staining

Nissl staining was performed to assess whether nasal gel HupA administration could affect the structure of the olfactory bulb. In brief, male APP/PS1 mice at 6 months of age were treated with nasal gel and nasal gel containing HupA, respectively, for 1 month. Mice were anaesthetized and killed by decapitation. The olfactory bulbs were removed and immersed in 4% paraformaldehyde for 24 h at 4 °C. Serial 10-μm coronal sections were prepared with a freezing microtome and stained with toluidine blue according to previous report (Kim *et al*, 2007). A total of 20 sections taken at equal intervals were selected (sections from 4.0 to 4.3 mm bregma) for the measurement of the area of olfactory granule cell layer (OGL) (Kim *et al*, 2007), using Image-pro Plus 6.0 analysis software.

BrdU Staining

Male APP/PS1 mice at 6 months of age were treated with nasal gel and nasal gel containing HupA, respectively, for 1 month. Afterwards, 5′-bromodeoxyuridine (BrdU) labeling was performed according to a previous report with minor modifications (Rochefort *et al*, 2002). Briefly, BrdU (B5002, Sigma) was administered intraperitoneally (50 mg/kg dissolved in 0.9% NaCl/0.07N NaOH) at 6 h intervals thrice per day for 3 continuous days. Mice were transcardially perfused with saline 2 h after the last injection. The brains were removed and cryostat sections (10 μm) were prepared. Sections were pretreated with 2 N HCl (Holick *et al*, 2008) for 2 h in a 37 °C water bath for DNA denaturation. Immunofluorescence staining and assessment of neurogenesis in the subventricular zone (SVZ) were performed by immunofluorescence assay with mouse anti-BrdU antibody (1 : 100, B8434, Sigma) as described previously (Kuhn *et al*, 1996). Five sections per animal were selected. The number and the area of BrdU-labeled cells in SVZ were measured with a confocal laser scanning microscope (SP2, Leica, Germany).

Evan's Blue Leakage Assay

APP/PS1 mice were treated with nasal gel HupA as mentioned above. Quantitation of Evan's blue (EB) leakage was carried out according to the protocol described previously (Lenzser *et al*, 2007; Lahoud-Rahme *et al*, 2009). Mice were intraperitoneally injected with 2% EB (50 mg/kg) 24 h after the last intranasal treatment. After 5 h, blood samples were collected from eyes. Then, mice were perfused with saline and the olfactory bulb, cortex, and hippocampus were separated. Samples were incubated with formamide for 72 h and centrifuged at 12 000 r.p.m. for 10 min. The absorbance of the supernatants was measured at 620 nm using a UV 1700 PharmaSpec ultraviolet spectrophotometer (Shimadzu). EB concentrations were calculated from standard curves. The value was expressed as EB/specimen weight normalized to plasma EB concentration.

AChE, ChAT, GSH-PX, CAT Activity, and MDA Content Measurements

The cortex of the left hemisphere of APP/PS1 mice treated with nasal gel and nasal gel containing HupA, at doses of 167 and 500 μg/kg, respectively, were weighed and a ninefold volume of phosphate-buffered saline was added and then the sample was ground gently at 4 °C. The detection of AChE and choline acetylase (ChAT) activity in the cortex of APP/PS1 mice was carried out by colorimetry according to the instructions for the corresponding kits (Jiancheng Biology, China). The absorbance was recorded at 520 and 324 nm for AChE and ChAT, respectively. Total protein levels were measured using a UV 1700 PharmaSpec ultraviolet spectrophotometer. Glutathione peroxidase (GSH-PX), CAT, and malondialdehyde (MDA) in the tissue homogenates were determined by colorimetry using suitable kits (Jiancheng Biology). The absorbance was recorded at 412, 240, and 532 nm for GSH-PX, CAT, and MDA, respectively.

Cell Culture, Drug Treatments, and MTT Assay

Human neuroblastoma SH-SY5Y cells stably transfected with APPsw or empty vector (neo) pCLNCXv.2 were made using Lipofectamine 2000 (Invitrogen) and selected by G418 resistance, as reported previously (Zhang *et al*, 2006a, b; Zheng *et al*, 2009). The cells were grown in Dulbecco's minimum essential medium (Gibco) supplemented with 10% heat-inactivated fetal bovine serum (Gibco) at 37 °C in a humidified incubator containing 5% CO_2, and were transferred to serum-free medium 2 h before drug treatments. The cells were treated with the protease inhibitor calphostin C or DKK-1 (R&D Systems) for 2 h and then treated with HupA for an additional 24 h. The cells were harvested for RT-PCR and western blot analysis.

Cell viability was measured in 96-well plates by quantitative colorimetric assay with MTT (Zheng *et al*, 2009; Yu *et al*, 2010). Briefly, after drug treatments, cells were incubated with medium containing 0.5 mg/ml MTT at 37 °C for 3 h and then treated with dimethylsulfoxide. The absorbance at 490 nm of each aliquot was determined using a microplate reader (TECAN). Cell viability was expressed

as the ratio of the signal obtained from the treated and control cultures.

Immunohistochemistry and Confocal Laser Scanning Microscopy

Serial 6-μm coronal sections were prepared and the routine ABC method was used to determine the distribution of Aβ in APP/PS1 mouse brain. Briefly, paraffin sections were dewaxed, rehydrated, and treated in 0.1 M Tris-HCl buffer (TBS, pH 7.4) containing 3% hydrogen peroxide (H_2O_2) for 10 min. Then, sections were boiled in TEG buffer for 5 min in a microwave oven. After rinsing, the sections were treated with 5% bovine serum albumin for 1 h, and incubated overnight with mouse anti-Aβ (1 : 500, A5213, Sigma) at 4 °C in a humidified chamber. Control sections were treated with identical solutions but without primary antibody. After rinsing, sections were incubated with biotinylated goat anti-mouse IgG (1 : 200) for 1 h, followed by amplification with streptavidin peroxidase for 1 h. After rinsing, the sections were treated with 0.025% 3,3-diaminobenzidine plus 0.0033% H_2O_2 in TBS for 5 min. The stained sections were dehydrated, cleared, and covered with neutral balsam. Sections were examined and images were collected using a light microscope equipped with a digital camera (Olympus). Quantification was carried out by taking micrographs of five sections per brain. The number of Aβ-positive plaques in the cortex and hippocampus was calculated, and the comparison between vehicle control and nasal gel HupA treatment groups was made using Image-Pro Plus 6.0 software. For Aβ burden analysis, the percentage of the sum of Aβ deposit areas compared with the total area of the cortex and hippocampus was quantified, and the data were analyzed with the above software.

For immunofluorescent staining, sections or culture cells were preincubated with normal donkey serum (1 : 20, Jackson ImmunoResearch Laboratory) for 1 h and then incubated overnight in mouse anti-OMP antibody (1 : 100, sc-67219, Santa Cruz), or a mixture of primary antibodies, mouse anti-Aβ (1 : 500), and rabbit anti-β-catenin (1 : 1000, 9582, Cell Signaling). Control sections were incubated with normal serum instead of primary antibodies. After rinsing, the sections or culture cells were incubated for 2 h with a mixture of secondary antibodies, Texas Red-conjugated donkey anti-rabbit IgG (1 : 50), and FITC-conjugated donkey anti-mouse IgG (1 : 50). After several rinses, the sections and culture cells were mounted using an anti-fading mounting medium and examined in a confocal laser scanning microscope. Excitation filters for FITC (488 nm) and Texas-Red (568 nm) were selected. Images were collected and processed using an Adobe Photoshop program.

Western Blot

Tissue homogenates of the olfactory bulb and cortex of APP/PS1 mice and culture cell lysates were centrifuged at 12 000 r.p.m. for 30 min at 4 °C. The supernatants were collected and total protein levels were measured using a UV 1700 PharmaSpec ultraviolet spectrophotometer. Proteins (50 μg) were separated on 10% SDS polyacrylamide gels and transferred to PVDF membranes (Millipore). The membranes were blocked with 5% non-fat milk in TBS containing 0.1% Tween-20 for 1 h and then incubated with a primary antibody for 2 h at room temperature. Antibodies used for western blot analysis included mouse anti-OMP (1 : 500, sc-67219; Santa Cruz), rabbit anti-GAP-43 (1 : 100, sc-33705; Santa Cruz), rabbit anti-ADAM10 (1 : 1000, AB19026; Millipore), rabbit anti-APP695 (1 : 4000, AB5352; Chemicon), rabbit anti-BACE1 (1 : 1000, B0681; Sigma), rat anti-PS1 (1 : 500, MAB1563; Millipore), mouse anti-sAPPα (1 : 500, 2B3, JP11088; IBM), mouse anti-sAPPβ (1 : 500, 6A1, JP10321; IBM), rabbit anti-APP-CTFs (1 : 4000, A8717; Sigma), rabbit anti-β-catenin (1 : 1000, 9582; Cell Signaling), rabbit anti-phospho-β-catenin (Ser33/37/Thr41) (1 : 1000, 9561; Cell Signaling), rabbit anti-GSK3α/β (1 : 1000, 27C10, 9315; Cell Signaling), rabbit anti-phospho-GSK3α/β (1 : 1000, 9327; Cell Signaling), and mouse anti-GAPDH (1 : 10000, 0811, KC-5G5; Kang Chen). Bound secondary antibodies were visualized by an enhanced chemiluminescence kit (Pierce) using Chem Doc XRS with Quantity One software (Bio-Rad). Blots were repeated at least three times for every condition. The band intensities were quantified using Image-pro Plus 6.0 analysis software.

RT-PCR

Tissue homogenates of the cortex of APP/PS1 mice and culture cell lysates were collected. Total RNA was isolated using Trizol reagent (Invitrogen) according to the manufacturer's protocol and the isolated RNA was quantied by UV spectroscopy at 260 nm. RNA purity was determined using the A260/A280 ratio (average >1.85). Total RNA of each sample was first reverse-transcribed into cDNA using the Reverse Transcription System (Promega). PCR amplification was performed with reagents from Promega. The cDNA solution was amplified with primers based on the human APP sequences. The primer sequences were: APP: 5′-GACTGACCACTCGACCAGGTTCTG-3′ (upstream), 5′-CTTG AAGTTGGATTCTCATACCG-3′ (downstream); GAPDH: 5′-ACGGATTTGGTCGTATTGGG-3′ (upstream), 5′-CGCTCCTG GAAGATGGTGAT-3′ (downstream). Amplification was performed as follows: APP: 35 cycles of 95 °C for 30 s, 62 °C for 30 s, and 72 °C for 30 s; GAPDH: 30 cycles of 95 °C for 45 s, 58 °C for 45 s, and 72 °C for 60 s. The PCR products were normalized in relation to standards of GAPDH mRNA.

Sandwich Elisa

The cortex of APP/PS1 mice treated with nasal gel and nasal gel containing HupA, at doses of 167 and 500 μg/kg, respectively, were placed in a 1 : 10 dilution of ice-cold lysis buffer containing an inhibitor protease cocktail. The samples were sonicated on ice for 1 min, allowed to stand overnight at 4 °C, and centrifuged at 12 000 r.p.m. for 30 min. The samples were then loaded on to 96-well plates and soluble Aβ was detected using soluble Aβ ELISA kits (KU0821E-10, Kuregen) and Aβ1-42 (KHB 3441, Invitrogen) in accordance with the manufacturer's instructions. The absorbance was recorded at 450 nm using a 96-well plate reader.

Statistical Analysis

All values were expressed as mean ± SEM. Statistical significance between nasal gel control and nasal gel HupA

treatment groups was determined by one-way analysis of variance (ANOVA) *post hoc* Bonferroni or Tamhane's T_2 test when appropriate. All other comparisons were analyzed by one-way ANOVA *post hoc* Fisher's PLSD. The $p<0.05$ was considered statistically significant.

RESULTS

Intranasal Administration with HupA Does Not Induce Significant Alteration of Olfactory Bulb Structure, Neurogenesis in SVZ, and Blood–Brain Barrier Permeability

We first evaluated the potential toxicity of intranasal administration of nasal gel HupA on mucocilia by examining the morphology of mucosal cilia by scanning electron microscopy. No obvious changes in the structure of mucocilia were found between the nasal gel (vehicle)- and nasal gel HupA-treated mouse nasal mucosa (Figure 1a, A1–A3), suggesting that the nasal mucocilia were not damaged after nasal administration of HupA at doses of 167 and 500 μg/kg once a day for a week.

We then assessed the olfactory bulb structure of APP/PS1 mice treated with nasal gel HupA by Nissl staining and olfactory marker protein (OMP) immunofluorescence. Nissl staining showed that the olfactory bulb exhibited similar histology in the vehicle- and nasal gel HupA-treated (167 and 500 μg/kg) mice (Figure 1a, B1–B3). Statistical analysis showed no significant difference in the area of OGL between vehicle and nasal gel HupA treatment groups (Figure 1b). OMP immunostaining showed that no obvious changes in the distribution and intensity of the immunofluorescence in the olfactory bulb were found between the vehicle- and nasal gel HupA-treated mice (Figure 1a, C1–C3). Furthermore, immunoblot showed that the expression levels of OMP and 43 kD growth-associated protein (GAP-43) did not exhibit marked difference between control and nasal gel HupA groups (OMP: $F(2,15)=1.082$, $p>0.05$, Figure 1c and d; GAP-43: $(F(2,15)=1.128$, $p>0.05$; Figure 1c and e).

We also examined the effects of intranasal administration of HupA or vehicle on olfactory bulb neurogenesis by BrdU staining. We failed to find BrdU-labeled cells in the olfactory bulb of control and nasal gel HupA mice treated with BrdU at 6 h intervals thrice per day for 3 continuous days (data not shown). However, BrdU-positive cells were found in the SVZ of control and nasal gel HupA-treated mice (Figure 1a, D1–D3). There were no significant differences in the number of BrdU-positive cells $(F(2,15)=1.741$, $p>0.05$; Figure 1f) and the area of BrdU in the SVZ $(F(2,15)=1.443$, $p>0.05$; Figure 1g).

Moreover, we evaluated whether long-term intranasal administration might compromise the blood–brain barrier (BBB) in APP/PS1 mouse brain by EB absorbance assay. As shown in Figure 1h, there was no significant difference in the leakage of EB in the olfactory bulb $(F(2,15)=0.171$, $p>0.05)$, cortex $(F(2,15)=0.107$, $p>0.05)$, and hippocampus $(F(2,15)=0.701$, $p>0.05$; Figure 1h).

Taken together, these data showed that nasal gel HupA administration did not induce significant alteration of olfactory bulb structure, neurogenesis in the SVZ, and BBB permeability, suggesting that no obvious toxicity of intranasal administration of HupA was found in the mouse brain.

Inhibition of AChE Activity and Antioxidative Effects of HupA in APP/PS1 Mouse Brain

To assess whether intranasal administration of nasal gel HupA retains its inhibitory effects on AChE activity, brain tissues of APP/PS1 mice treated with nasal gel HupA for 4 months were subjected to colorimetric tests to determine the AChE and ChAT activity in the brain. HupA treatment dose dependently reduced AChE levels by $90.61\pm3.41\%$ $(p<0.05)$ and $87.61\pm4.21\%$ $(p<0.01)$ at a dose of 167 and 500 μg/kg, respectively $(F(2,15)=6.777$, $p<0.05$; Figure 2a), and increased ChAT levels by $111.90\pm12.29\%$ (167 μg/kg; $p>0.05$) and $123.13\pm11.50\%$ (500 μg/kg; $p<0.05$), respectively $(F(2,15)=9.628$, $p<0.05$; Figure 2b). These data suggest that intranasal administration of HupA dose dependently increases ChAT activity, which is a well-known effect of HupA using the traditional administration modes, such as intravenous and oral administration.

We then analyzed the effects of HupA on modulating the activities of antioxidant enzymes and oxidative production of MDA in the APP/PS1 transgenic mouse brain. Nasal gel HupA treatment increased the levels of GSH-PX to $140.49\pm6.04\%$ (167 μg/kg; $p<0.01$) and $159.91\pm11.12\%$ (500 μg/kg; $p<0.01$), respectively $(F(2,15)=23.391$, $p<0.05$; Figure 2c), and increased the activity of CAT to $114.28\pm5.29\%$ (167 μg/kg; $p<0.05$) and $124.34\pm7.09\%$ (500 μg/kg; $p<0.01$), respectively $(F(2,15)=16.971$, $p<0.05$, Figure 2d). Meanwhile, HupA reduced oxidative production of MDA to $88.88\pm1.95\%$ (167 μg/kg; $p<0.05$) and $87.42\pm5.49\%$ (500 μg/kg; $p<0.05$), respectively, compared with control $(F(2,15)=11.887$, $p<0.05$; Figure 2e). Collectively, nasal gel HupA enhanced the activities of antioxidative enzymes and subsequently reduced the oxidative production in APP/PS1 mouse brain.

HupA Reduces Aβ Burden and Inhibits Aβ Generation in APP/PS1 Mouse Brain

We investigated whether nasal gel HupA could reduce Aβ deposition in APP/PS1 mouse brain. Brain sections of APP/PS1 mice treated with nasal gel HupA for 4 months were subjected to immunohistochemical analysis. Both the number and size of the Aβ-immonoreactive neuritic plaques were dose dependently reduced in the cortex and hippocampus after intranasal treatment of HupA (Figure 3a). Statistical analysis showed that HupA treatment significantly reduced the number of Aβ plaques by 77.52 ± 12.94 and $37.07\pm8.06\%$ at a dose of 167 and 500 μg/kg, respectively, in the cortex $(F(2,15)=70.263$, $p<0.05)$, and $45.13\pm10.46\%$ (167 μg/kg; $p<0.01$) and $26.73\pm7.15\%$ (500 μg/kg; $p<0.01$), respectively, in the hippocampus compared with the vehicle control $(F(2,15)=27.656$, $p<0.05$; Figure 3b). The areas of neuritic plaques of the HupA treatment groups were reduced by $72.07\pm10.56\%$ (167 μg/kg; $p<0.01$) and $27.34\pm4.94\%$ (500 μg/kg; $p<0.01$) in the cortex $(F(2,15)=193.938$, $p<0.05)$, and $66.04\pm12.66\%$ (167 μg/kg; $p<0.01$) and $41.66\pm6.23\%$ (500 μg/kg; $p<0.01$) in the hippocampus $(F(2,15)=44.254$, $p<0.05$; Figure 3c), respectively.

Next, we measured the soluble Aβ level in the cortex of the transgenic mouse brain by sandwich ELISA. After treatment with nasal gel HupA for 4 months, the levels of Aβ1-40 were reduced by $88.84\pm7.35\%$ (167 μg/kg; $p<0.05$) and

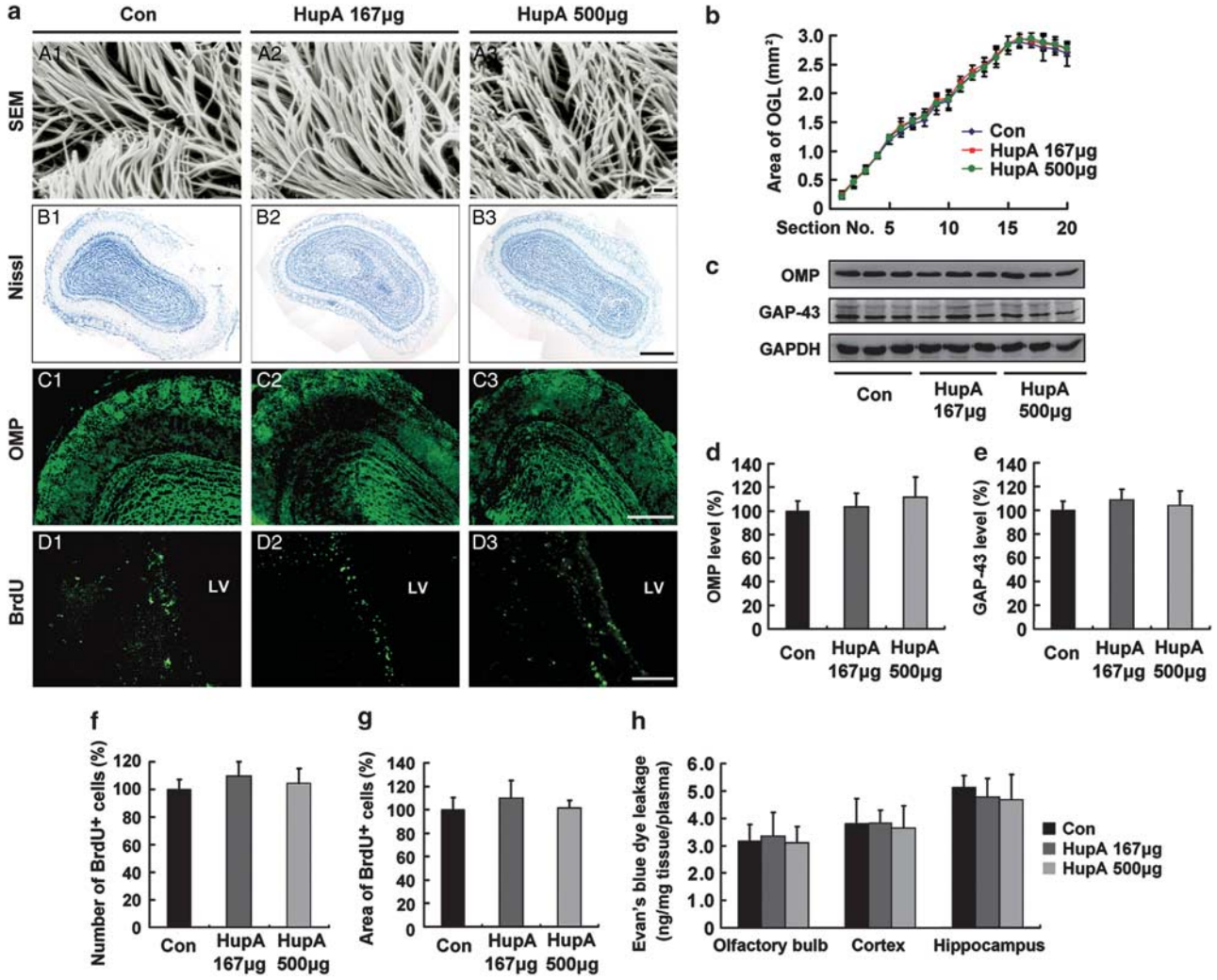

Figure 1 Evaluation of the potential toxicity of intranasal administration of nasal gel HupA on olfactory bulb (OB) and neurogenesis in the subventricular zone (SVZ) of mice. (a; A1–A3) Scanning electron microscope (SEM) photographs showing no marked changes in the structure of nasal mucocilia between C57BL/6 mice given nasal gel (A1), and nasal gel containing HupA at a dose of 167 μg/kg (A2) and 500 μg/kg (A3), respectively, for 7 days. Scale bar = 1 μm. (B1–D3) APP/PS1 mice were treated with vehicle and nasal gel HupA, respectively, for 1 month. Nissl staining of OB exhibited similar histology between vehicle group (B1) and nasal gel HupA at doses of 167 μg/kg (B2) and 500 μg/kg groups (B3). Scale bar = 200 μm. (C1–C3) Immunostaining images showing the distribution and expression of olfactory marker protein (OMP) in OB of APP/PS1 mice. No marked changes were found between vehicle- and HupA-treated groups. Scale bar = 100 μm. (D1–D3) BrdU immunofluorescent staining showed a similar neurogenesis in SVZ between vehicle and nasal gel HupA groups. Scale bar = 50 μm. (b) Measurement of the area of olfactory granule cell layer (OGL) in serial sections of Nissl staining. No significant differences were found between vehicle- and HupA-treated transgenic mice. (c) Western blot showed the protein levels of OMP and GAP-43 in the OB of vehicle- and HupA-treated APP/PS1 mice. GAPDH was used as an internal control. (d, e) Quantification of the protein levels of OMP (d) and GAP-43 (e) in the OB. Intranasal administration of HupA did not alter the expression levels of OMP and GAP-43, compared with controls. (f, g) Quantification of the number (f) and the area (g) of BrdU-labeled cells in SVZ showed no significant difference between control and HupA groups. (h) Leakage of Evan's blue (EB) showed that nasal gel HupA treatment did not significantly change the EB absorbance in the OB, cortex, and hippocampus in APP/PS1 mice. All values are mean ± SEM ($n = 6$).

$80.87 \pm 8.93\%$ (500 μg/kg; $p < 0.05$), respectively ($F(2, 15) = 12.329$, $p < 0.05$; Figure 3d), and the levels of Aβ1-42 were reduced by $76.89 \pm 10.78\%$ (167 μg/kg; $p < 0.01$) and $52.21 \pm 10.14\%$ (500 μg/kg; $p < 0.01$), respectively ($F(2, 15) = 19.267$, $p < 0.05$; Figure 3e) compared with the control group.

HupA Enhances Nonamyloidogenic Processing of APP in APP/PS1 Mouse Brain

To verify the effects of HupA on APP processing, we first measured the levels of APP mRNA and APP695 protein in APP/PS1 mouse brain following treatment with nasal gel HupA for 4 months. RT-PCR results showed that there were no significant differences in APP mRNA levels between vehicle control and HupA treatment groups in APP/PS1 mouse brain ($F(2, 15) = 2.158$, $p > 0.05$; Figure 4a and b). However, immunoblot analysis revealed that HupA treatment dose dependently reduced the levels of APP695 protein by $71.22 \pm 15.16\%$ (167 μg/kg; $p < 0.05$) and $59.28 \pm 5.60\%$ (500 μg/kg; $p < 0.01$), respectively, compared with the control group ($F(2, 15) = 14.349$, $p < 0.05$; Figure 4c and d).

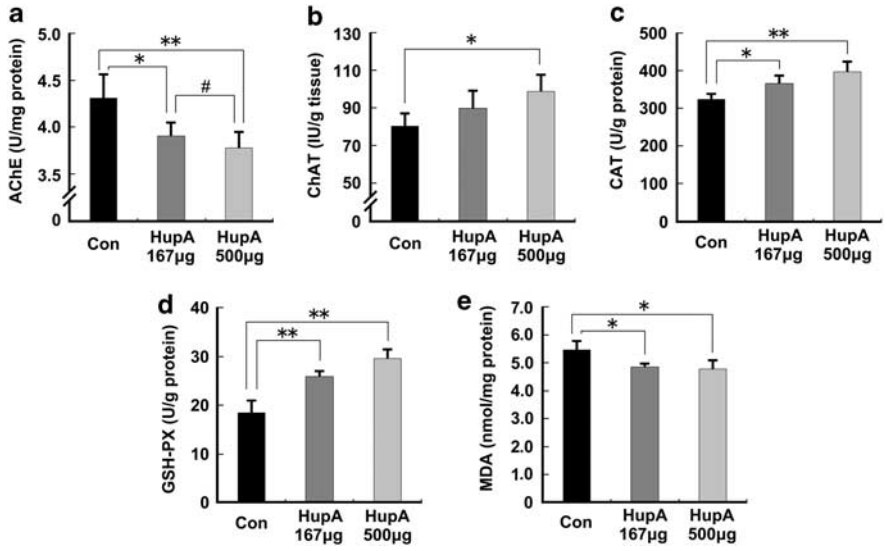

Figure 2 Effects of nasal gel HupA on AChE and antioxidant enzyme activity in the cortex of APP/PS1 mice. APP/PS1 transgenic mice at the age of 6 months were treated with nasal gel HupA at a dose of 167 and 500 μg/kg, respectively, for 4 months. AChE and ChAT activity of brain cortex tissue homogenate were measured by AChE and ChAT assay kits. (a) Administration of HupA significantly reduced AChE activity in the mouse brain. (b) HupA dose dependently increased ChAT activity in the mouse brain. (c) HupA significantly increased the activity of the detected antioxidant enzymes, CAT and GSH-PX (d), in APP/PS1 mouse brain. (e) Nasal gel HupA significantly reduced the production of MDA in the mouse brain. All values are mean ± SEM ($n = 6$). $^{*}p < 0.05$, $^{**}p < 0.01$, $^{\#}p < 0.05$.

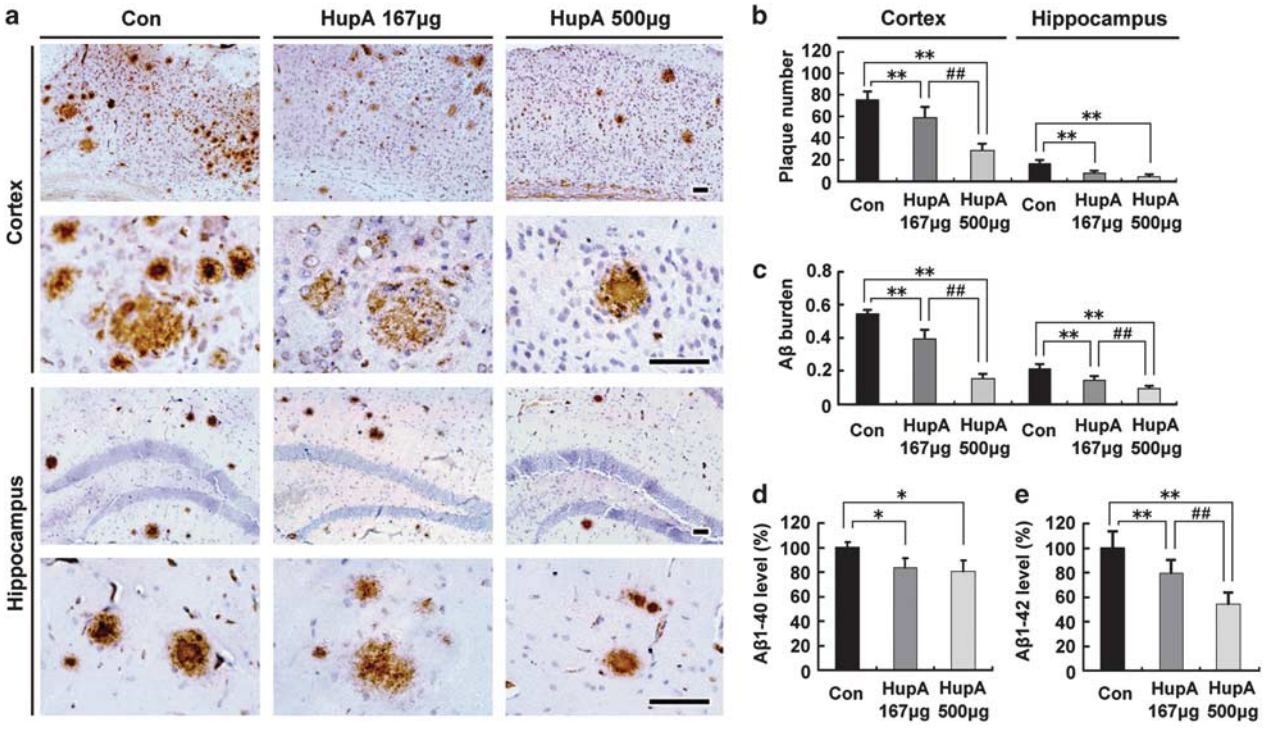

Figure 3 Nasal gel HupA treatment significantly reduces Aβ plaque formation and soluble Aβ production in APP/PS1 mouse brain. (a) Aβ immunoreactive neuritic plaques in the cortex and hippocampus of transgenic mice treated with nasal gel and nasal gel HupA at a dose of 167 and 500 μg/kg, respectively. The number of Aβ-positive plaques was significantly reduced in HupA-treated mice compared with controls. Scale bar = 60 μm. (b, c) Quantification of the number of Aβ-positive plaques (b) and Aβ burden (c) in the cortex and hippocampus of APP/PS1 mice treated with HupA. HupA significantly reduced the plaque number and Aβ burden in the brain in a dose-dependent manner. (d, e) ELISA results showed that administration of nasal gel HupA induced a dose-dependent decrease in soluble Aβ production in the cortex of APP/PS1 mice. All values are mean ± SEM ($n = 6$). $^{*}p < 0.05$, $^{**}p < 0.01$, $^{\#\#}p < 0.01$.

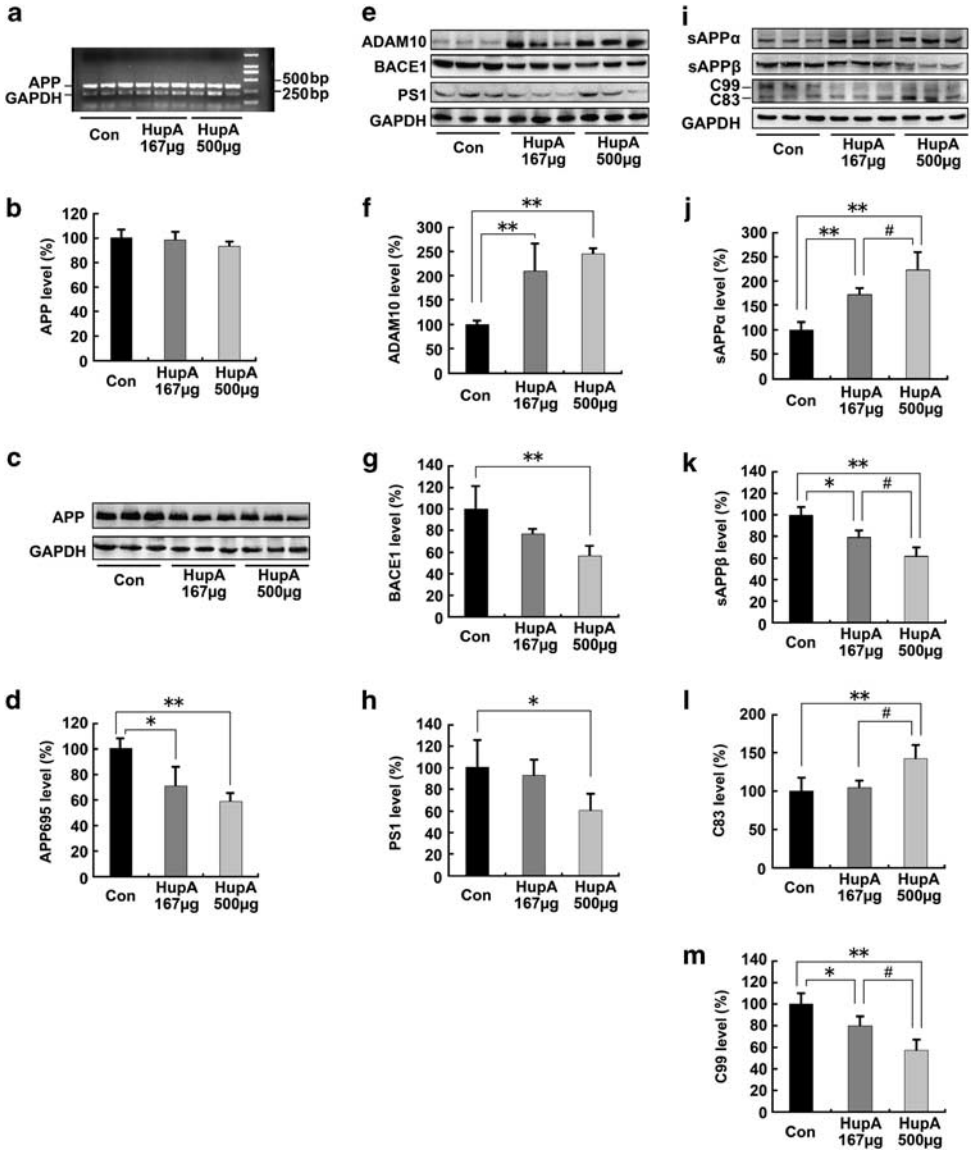

Figure 4 Nasal gel HupA enhances the nonamyloidogenic pathway in APP/PS1 mouse brain. (a) Expression levels of APP mRNA were detected by RT-PCR in the brain of APP/PS1 transgenic mice treated with nasal gel and nasal gel HupA at a dose of 167 and 500 μg/kg, respectively. GAPDH was used as an internal reference gene. (b) HupA-treated and vehicle control APP/PS1 mice exhibited a similar APP mRNA level. (c) Western blots showed the expression levels of APP695 protein in the vehicle- and HupA-treated transgenic mouse brain. GAPDH was used as an internal control. (d) The protein levels of APP695 were significantly reduced in the nasal gel HupA-treated mouse brain compared with the vehicle controls. (e) The expression levels of APP cleavage enzymes, including ADAM10, BACE1, and PS1, were examined by western blot analysis. (f–h) Analysis results showed that the protein levels of ADAM10 were significantly increased (f), whereas the levels of BACE1 were markedly reduced in the brain of nasal gel HupA-treated mice (g). HupA treatment reduced the expression levels of PS1 protein in a dose-dependent manner, compared with vehicle controls (h). (i) Immunoblotting showed the expression levels of APP cleavage fragments, including sAPPα, sAPPβ, C83, and C99, in the vehicle- and HupA-treated transgenic mouse brain. (j–m) Quantification of sAPPα, sAPPβ, C83, and C99 generation in the brain of the APP/PS1 mouse. Nasal gel HupA treatment significantly increased the levels of sAPPα (j) and C83 (l) and reduced the levels of sAPPβ (k) and C99 (m) in a dose-dependent manner. All values are mean ± SEM ($n = 6$). $^{*}p < 0.05$, $^{**}p < 0.01$, $^{\#}p < 0.05$.

We then investigated whether nasal gel HupA was involved in APP cleavage. The APP cleavage enzymes and cleavage fragments in HupA-treated transgenic mouse brain were detected by western blot analysis (Figure 4e and i). HupA significantly increased the expression level of a disintegrin and metallopetidase 10 (ADAM10) by 210.05 ± 57.43% (167 μg/kg; $p < 0.01$) and 245.02 ± 11.41% (500 μg/kg; $p < 0.01$), respectively ($F(2, 15) = 14.833$, $p < 0.05$; Figure 4f). On the other hand, HupA dose dependently reduced the level of the β-site of APP-cleaving enzyme (BACE1) by 76.93 ± 4.77% (167 μg/kg; $p > 0.05$) and 56.65 ± 9.20% (500 μg/kg; $p < 0.01$) ($F(2, 15) = 7.406$, $p < 0.05$; Figure 4g). Furthermore, HupA reduced the level of PS1 by 92.81 ± 13.46% (167 μg/kg; $p > 0.05$) and 62.09 ± 12.00% (500 μg/kg; $p < 0.05$) compared with vehicle controls ($F(2, 15) = 8.210$, $p < 0.05$; Figure 4h).

In HupA-treated transgenic mouse brain, the protein level of sAPPα was increased by 171.91 ± 13.47% (167 μg/kg; $p < 0.01$) and 222.88 ± 36.00% (500 μg/kg; $p < 0.01$) ($F(2, 15) = 26.780$, $p < 0.05$; Figure 4j), in parallel with a decreased

release of sAPPβ by 79.78 ± 6.33% (167 μg/kg; $p<0.05$) and 62.19 ± 8.38% (500 μg/kg; $p<0.01$) ($F(2,15)=24.423$, $p<0.05$; Figure 4k). HupA treatment led to an increased level of C83 by 104.73 ± 9.36% (167 μg/kg; $p>0.05$) and 142.65 ± 17.22% (500 μg/kg; $p<0.01$) ($F(2,15)=9.279$, $p<0.05$; Figure 4l), and a decreased level of C99 by 79.92 ± 9.18% (167 μg/kg; $p<0.05$) and 57.32 ± 10.15% (500 μg/kg; $p<0.01$) ($F(2,15)=18.850$, $p<0.05$; Figure 4m), compared with vehicle controls. Taken together, these results suggest that the α-secretase cleavage activity is markedly increased following administration of nasal gel HupA and, thus, this promotes nonamyloidogenic processing of APP and attenuates cerebral amyloidosis in APP/PS1 mouse brain.

HupA Inhibits GSK3 and Stabilizes the Level of β-Catenin in APP/PS1 Mouse Brain

As recent *in vitro* studies have shown that AChE–Aβ toxicity may destroy the Wnt pathway and cause cholinergic neuronal loss (Inestrosa *et al*, 2000, 2004, 2005), we investigated whether HupA could target the Wnt signaling cascades by examining the expression levels of both GSK3β and β-catenin, the two key components in the Wnt signaling pathway.

We first detected the protein levels of both GSK3β and phosphorylated GSK3β (p-GSK3β) in HupA-treated APP/PS1 mouse brains with western blot analyses (Figure 5a). HupA treatment did not affect the levels of total GSK3β protein ($F(2,15)=3.806$, $p>0.05$; Figure 5b), but the levels of p-GSK3β were dose dependently increased by 150.56 ± 27.94% ($p>0.05$) and 279.93 ± 36.42% ($p<0.05$) at a dose of 167 and 500 μg/kg, respectively ($F(2,15)=44.722$, $p<0.05$; Figure 5c). Consequently, treatment with HupA increased the ratio of p-GSK3β/GSK3β by 156.52 ± 66.83% (167 μg/kg; $p>0.05$) and by 213.07 ± 39.50% (500 μg/kg; $p<0.05$) ($F(2,15)=8.508$, $p<0.05$; Figure 5d). We also investigated whether HupA affected the activity of GSK3α. The levels of total GSK3α protein were not altered ($F(2,15)=1.938$, $p>0.05$; Figure 5e), but the levels of p-GSK3α were increased by 159.99 ± 28.87% ($p<0.01$) and by 260.25 ± 23.88% ($p<0.01$) at a dose of 167 and 500 μg/kg, respectively ($F(2,15)=52.075$, $p<0.05$; Figure 5f). The ratio of p-GSK3α/GSK3α was also increased by 144.29 ± 33.22% (167 μg/kg; $p<0.05$) and 251.52 ± 61.66% (500 μg/kg; $p<0.01$) compared with that in the control group ($F(2,15)=21.678$, $p<0.05$; Figure 5g). These data suggest that treatment with nasal gel HupA inactivates both GSK3β and GSK3α in transgenic mouse brain in a dose-dependent manner.

Next, we analyzed the distribution and expression of β-catenin in transgenic mouse brain with double immunofluorescence labeling of Aβ and β-catenin. Confocal microscopic observation showed that β-catenin immunofluorescence was predominantly observed around the Aβ-positive plaques in the transgenic mouse brain (Figure 6a). High-magnification images clearly showed that most of the β-catenin-positive products were located in the cell bodies with a large-sized DAPI-stained nucleus (Figure 6a), suggesting a neuronal cell localization of β-catenin in the mouse brain. Double labeling of β-catenin and NeuN (for neurons), GFAP (for astrocytes), or Iba-1 (for microglias) confirmed this notion (data not shown). Most importantly, HupA treatment markedly increased the density of β-catenin immunofluorescence around the Aβ-positive plaques in a dose-dependent manner (Figure 6a). These findings suggest that HupA may protect against Aβ-induced neuronal death through activation of β-catenin.

We then measured the protein levels of both β-catenin and p-β-catenin after intranasal treatment of HupA in APP/PS1 mouse brain. Immunoblot results showed that nasal gel HupA increased the levels of β-catenin ($F(2,15)=11.509$, $p<0.05$; Figure 6b), and β-catenin increased by 172.01 ± 32.14% (167 μg/kg; $p<0.05$) and 210.21 ± 41.04% (500 μ/kg; $p<0.01$) compared with the control (Figure 6c).

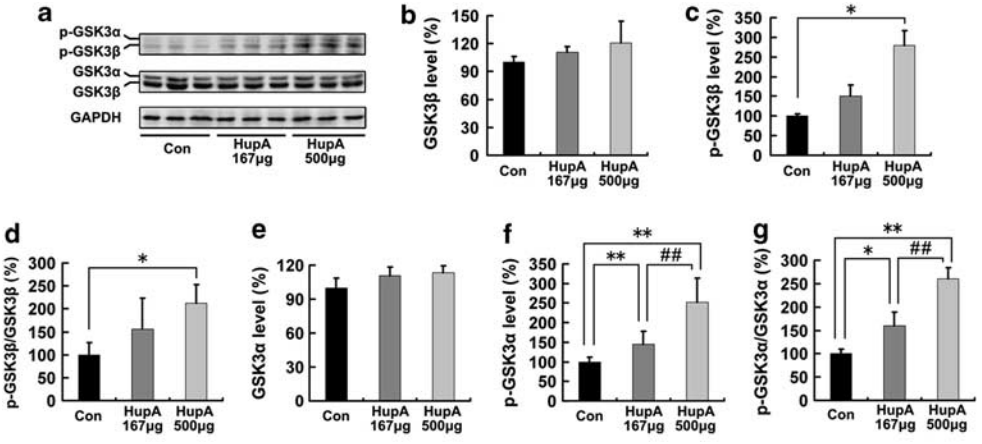

Figure 5 Nasal gel HupA upregulates the phosphorylation levels of GSK3α/β in APP/PS1 mouse brain. (a) Western blots showing the expression levels of total GSK3α/β and p-GSK3α/β in APP/PS1 transgenic mouse brain after HupA treatments. GAPDH was used as an internal control. (b–d) Quantification of the levels of GSK3β and p-GSK3β in the brain of the APP/PS1 mouse. There were no significant differences in total GSK3β levels between vehicle- and HupA-treated mouse brain (b). However, the levels of p-GSK3β were significantly increased after 500 μg HupA treatment (c). Moreover, the ratio of p-GSK3β/GSK3β was significantly increased in 500 μg nasal gel HupA-treated mice (d). (e–g) Quantification of the levels of GSK3α and p-GSK3α in the brain of the APP/PS1 mouse. Administration of HupA did not affect the total protein levels of GSK3α (e). The levels of p-GSK3α were markedly increased after HupA treatment (f). Nasal gel HupA induced a dose-dependent increase in the ratio of p-GSK3α/GSK3α in the transgenic mouse brain (g). All values are mean ± SEM ($n=6$). $^{*}p<0.05$, $^{**}p<0.01$, $^{\#\#}p<0.01$.

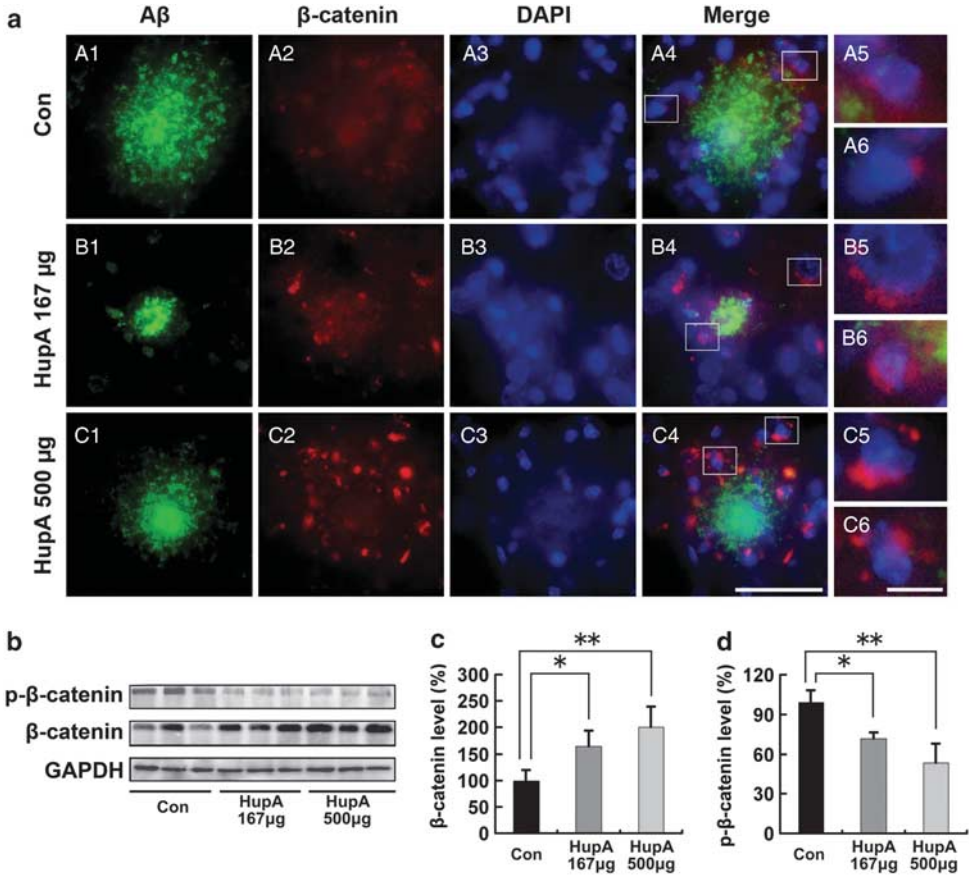

Figure 6 Nasal gel HupA enhances the level of β-catenin in APP/PS1 mouse brain. (a) Confocal microscopic images showing the distribution of β-catenin in the HupA-treated transgenic mouse brain with double immunofluorescent staining of Aβ (A1, B1, and C1) and β-catenin (A2, B2, and C2). Counterstaining of DAPI was used to show the nucleus (A3, B3, and C3). At the merged images from the three channels, it was evident that the β-catenin immunoproducts were located around the Aβ-positive neuritic plaques (A4, B4, and C4), and that the β-catenin immunofluorescence was mainly located in the neuronal cell bodies (A5, A6, B5, B6, C5, and C6). Figure B5 shows a typical neuron with a large nucleus and containing intense β-catenin immunofluorescence in the cell body. In the vehicle-treated control mouse brain, the density of β-catenin immunofluorescence was very weak (A2), whereas it was very intense in the HupA-treated transgenic mouse brain (B2 and C2). Scale bar = 50 μm (C4) and 10 μm (C6). (b) Protein levels of β-catenin and p-β-catenin (Ser33/37/Thr41) were examined by western blot in the brain of transgenic mice. GAPDH was used as an internal control. (c, d) Analysis results showed that the protein levels of total β-catenin were markedly increased (c), whereas the levels of p-β-catenin were significantly decreased in HupA-treated mice compared with controls (d). All values are mean ± SEM ($n = 6$). *$p < 0.05$, **$p < 0.01$.

Furthermore, HupA treatment significantly decreased the levels of p-β-catenin by 72.24 ± 5.06% (167 μg/kg; $p < 0.05$) and 53.83 ± 14.63% (500 μg/kg; $p < 0.01$), respectively ($F(2, 15) = 19.654$, $p < 0.05$; Figure 6d). Collectively, these data indicate that nasal gel HupA stabilizes the level of β-catenin in APP/PS1 mouse brain.

HupA Enhances Nonamyloidogenic Processing of APP *In Vitro*

To examine the effect of HupA on APP processing *in vitro*, APPsw-transfected SH-SY5Y cells were treated with HupA. The MTT assay showed that 0–10 μM HupA did not exhibit any significant toxic effects on the cells (Figure 7a), and dose dependently increased the levels of sAPPα after treatment for 18 h ($F(3, 12) = 6.705$, $p < 0.05$) and 24 h ($F(3, 12) = 10.766$, $p < 0.05$; Figure 7b). Accordingly, treatment with 10 μM HupA for 24 h was chosen for the subsequent *in vitro* experiments.

We then examined the levels of APP cleavage enzymes and APP fragments in HupA-treated APPsw cells using western blot analyses (Figure 7d and h). APPsw cells treated with 10 μM HupA showed an increased level of ADAM10, by 118.39 ± 3.64% ($p < 0.05$; Figure 7e), and a reduced level of BACE1, by 70.13 ± 7.84% ($p < 0.01$), in APPsw cells (Figure 7f). No statistically significant changes in the protein levels of PS1 were detected between HupA-treated and control cells ($F(5, 24) = 2.017$, $p > 0.05$; Figure 7g). Moreover, HupA treatment markedly increased the level of sAPPα by 166.56 ± 9.80% ($p < 0.01$; Figure 7i) and reduced the level of sAPPβ by 57.18 ± 7.45% ($p < 0.01$; Figure 7j). HupA treatment significantly increased the level of C83 by 110.81 ± 7.8% ($p < 0.05$; Figure 7k), but reduced the release of C99 by 78.12 ± 5.54% ($p < 0.01$; Figure 7l).

HupA Reverses PKC- and Wnt-Inhibitor-Induced Inhibition of Nonamyloidogenic Processing of APP *In Vitro*

Previous studies have suggested that GSK3 regulates Aβ formation (Pei *et al*, 1999; Phiel *et al*, 2003; Muyllaert *et al*, 2006), and protein kinase C (PKC) is involved in the

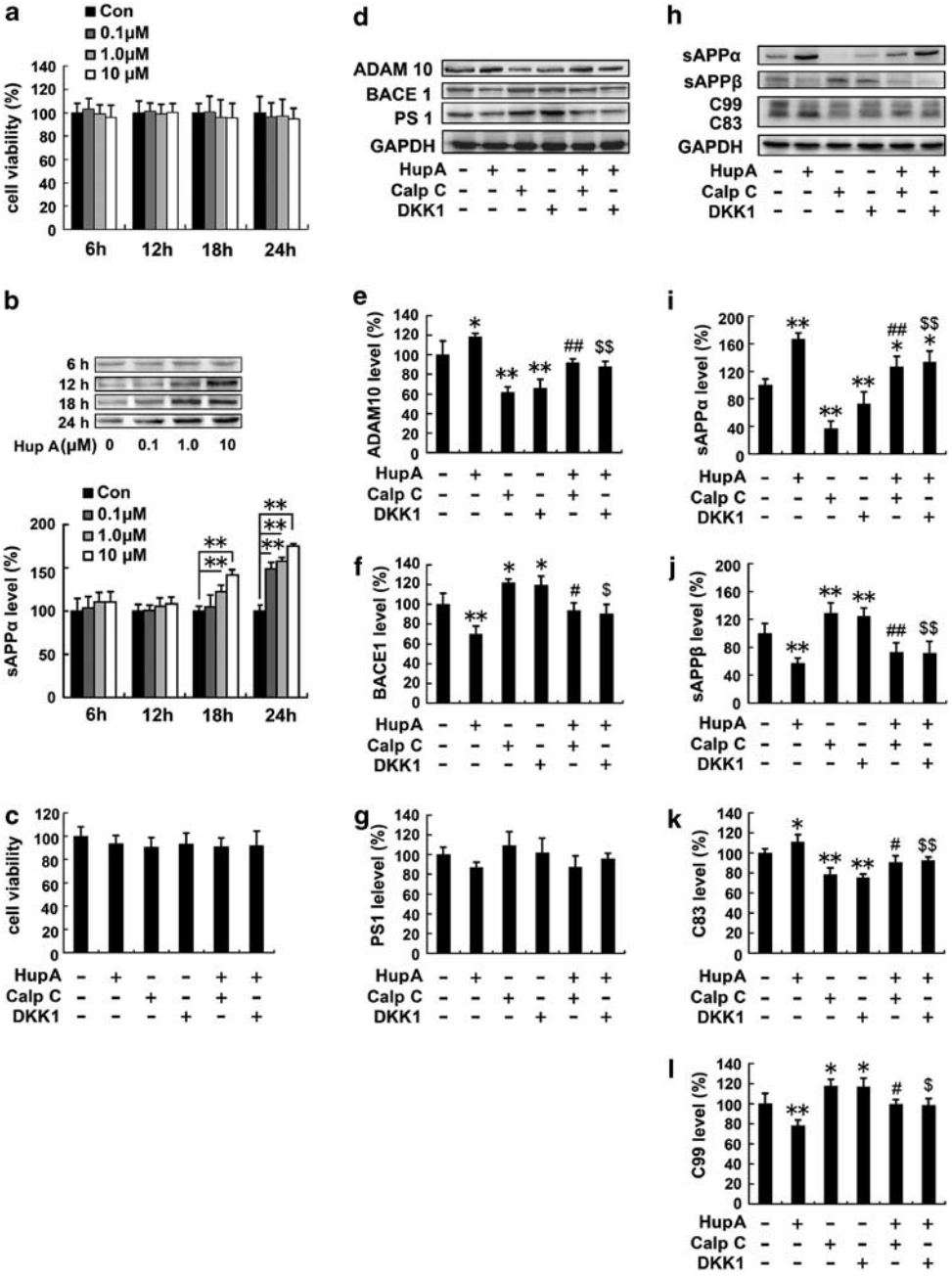

Figure 7 HupA enhances nonamyloidogenic processing of APP in SH-SY5Y cells transfected with APPsw. (a) MTT results indicated that 0–10 μM HupA did not have any significant toxic effects on the cells at different periods of treatment. (b) Immunoblotting detection of the protein levels of sAPPα in 0, 0.1, 1.0, or 10 μM HupA-treated APPsw cells. GAPDH was used as an internal control. Analysis results showed that HupA increased sAPPα release in a dose- and time-dependent manner. (c) Representative MTT results showing that there were no significant changes in cell viability in APPsw cells exposed to 10 μM HupA, 1 μM calphostin C (PKC inhibitor), and 50 ng/ml DKK-1 (Wnt signaling inhibitor). Thus, the above doses of HupA and inhibitors were used in the subsequent experiments in culture cells. (d) Western blot analyses were carried out to examine the expression levels of APP cleavage enzymes, ADAM10, BACE1, and PS1, in APPsw cells. (e, f) HupA significantly increased the ADAM10 level and decreased the level of BACE1. There was a significant decrease in the ADAM10 level and an increase in the BACE1 level in cultures treated with calphostin C or DKK1, whereas the levels of ADAM10 and BACE1 were reversed when cultures were preincubated with calphostin C or DKK1 followed by HupA. (g) There were no significant changes in the PS1 level in drug-treated cells compared with controls. (h) Western blots showing the expression levels of APP cleavage fragments in APPsw cells. (i–l) HupA significantly increased the levels of sAPPα and C83 and decreased the levels of sAPPβ and C99. Calphostin C and DKK1 significantly reduced the levels of sAPPα and C83 and increased the levels of sAPPβ and C99, whereas HupA reversed the inhibitor-induced reduction of sAPPα and C83 and increased that of sAPPβ and C99. All results are presented as the mean ± SEM of at least three independent experiments. $^{*}p<0.05$, $^{**}p<0.01$ *vs* control group; $^{\#}p<0.05$, $^{\#\#}p<0.01$ *vs* calphostin C-treated group; $^{\$}p<0.05$, $^{\$\$}p<0.01$ *vs* DKK1-treated group.

inactivation of GSK-3β in the Wnt signaling pathway (Cook *et al*, 1996; Sheldahl *et al*, 1999; Chen *et al*, 2000). To further investigate the underlying mechanism of the effect of HupA on the nonamyloidogenic processing of APP, we examined the expression levels of APP cleavage enzymes and fragments in APPsw cells preincubated with the PKC

inhibitor calphostin C (1 μM) and the Wnt signaling inhibitor DKK-1 (50 ng/ml) followed by HupA treatment. The doses of inhibitors were selected based on the MTT assay (Figure 7c).

Immunoblotting showed that calphostin C or DKK1 treatment significantly reduced the levels of ADAM10 to 61.73 ± 5.56% ($p < 0.01$) and 66.04 ± 9.23% ($p < 0.01$) ($F(5, 24) = 20.938$, $p < 0.05$) and increased the levels of BACE1 to 122.11 ± 3.72% ($p < 0.05$) and 119.70 ± 8.84% ($p < 0.05$), respectively ($F(5, 24) = 16.227$, $p < 0.05$), compared with controls (Figure 7d–f). However, HupA treatment reversed the changes in ADAM10 to 148.75 ± 7.22% (calphostin C + HupA) compared with the calphostin C-treated group ($p < 0.01$), and 132.90 ± 8.71% (DKK1 + HupA) compared with DKK1 treatment ($p < 0.01$). HupA treatment reversed the changes in BACE1 to 77.10 ± 5.99% (calphostin C + HupA) compared with the calphostin C-treated group ($p < 0.05$), and 75.65 ± 7.83% (DKK1 + HupA) compared with DKK1 treatment ($p < 0.05$), respectively (Figure 7d–f).

The levels of sAPPα and C83 in cultures treated with inhibitors were significantly reduced by 36.96 ± 11.04% (calphostin C; $p < 0.01$) and 73.03 ± 11.28% (DKK1; $p < 0.01$) ($F(5, 24) = 34.333$, $p < 0.05$; Figure 7i), and by 78.69 ± 6.72% (calphostin C; $p < 0.01$) and 75.38 ± 3.89% (DKK1; $p < 0.01$) ($F(5, 24) = 15.992$, $p < 0.05$; Figure 7k), respectively, compared with the control group. However, HupA treatment reversed the levels of sAPPα to 342.90 ± 42.39% (calphostin C + HupA) compared with the calphostin C-treated group ($p < 0.01$), and 182.63 ± 22.62% (DKK1 + HupA) compared with DKK1 treatment ($p < 0.01$). Meanwhile, HupA treatment reversed the level of C83 to 115.19 ± 4.95% (calphostin C + HupA) compared with calphostin C treatment ($p < 0.05$), and 122.43 ± 5.08% (DKK1 + HupA) compared with the DKK1-treated group ($p < 0.01$; Figure 7i and k).

However, the levels of sAPPβ and C99 in cultures treated with inhibitors significant increased by 129.03 ± 14.96% (calphostin C; $p < 0.01$) and 125.07 ± 11.49% (DKK1; $p < 0.01$) ($F(5, 24) = 14.905$, $p < 0.05$; Figure 7j), and by 117.65 ± 6.46% (calphostin C; $p < 0.05$) and 116.88 ± 8.68% (DKK1; $p < 0.05$) ($F(5, 24) = 11.765$, $p < 0.05$; Figure 7l) compared with controls. In cultures preincubated with inhibitors and then treated with HupA, the levels of sAPPβ were reversed to 56.62 ± 10.40% (calphostin C + HupA) compared with the calphostin C-treated group ($p < 0.01$), and 57.14 ± 13.55% (DKK1 + HupA) compared with DKK1 treatment ($p < 0.01$). Meanwhile, HupA treatment reversed the level of C99 to 84.44 ± 4.15% (calphostin C + HupA) compared with the calphostin C-treated group ($p < 0.05$), and 84.27 ± 5.92% (DKK1 + HupA) compared with the DKK1-treated group ($p < 0.05$). These results show that HupA reverses PKC- and Wnt-inhibitor-induced inhibition of nonamyloidogenic processing of APP *in vitro*.

HupA Inactivates GSK3 and Stabilizes the Level of β-Catenin *In Vitro*

We extended our experiments to determine whether HupA could modulate the Wnt signaling cascades *in vitro*. We first examined the expression levels of GSK3 in APPsw cells pretreated with calphostin C or DKK-1 followed by treatment with HupA. As shown in Figure 7, the protein levels of total GSK3α/β were not affected by drug treatments, but the levels of p-GSK3α/β were markedly altered (Figure 8a). The analysis showed that the ratio of p-GSK3β/GSK3β in cultures treated with inhibitors significantly decreased by 64.28 ± 7.88% (calphostin C) and 62.96 ± 3.88% (DKK1) compared with controls ($p < 0.01$; Figure 8b), whereas HupA treatment reversed the ratio of p-GSK3β/GSK3β to 125.53 ± 14.70% (calphostin C + HupA) compared with the calphostin C treatment group ($p < 0.01$), and 129.98 ± 10.39% (DKK1 + HupA) compared with DKK1 treatment ($p < 0.01$), respectively ($F(5, 24) = 36.089$, $p < 0.05$; Figure 8b). Furthermore, calphostin C or DKK1 treatment significantly reduced the ratio of p-GSK3α/GSK3α to 61.47 ± 4.76 and 62.15 ± 11.05%, respectively, compared with controls ($p < 0.01$; Figure 8c), whereas HupA treatment increased the levels of p-GSK3α/GSK3α to 158.10 ± 21.46% (calphostin C + HupA) compared with calphostin C treatment ($p < 0.01$), and 170.09 ± 10.29% (DKK1 + HupA) compared with the DKK1-treated group ($p < 0.01$) ($F(5, 24) = 37.423$, $p < 0.05$; Figure 8c).

We next analyzed the distribution and expression of β-catenin in APPsw cells with double immunofluorescence labeling of Aβ and β-catenin. Consistent with our *in vivo* data, confocal microscopy results showed that HupA treatment markedly increased the β-catenin immunofluorescence in APPsw cells (Figure 9a, B2). Furthermore, both

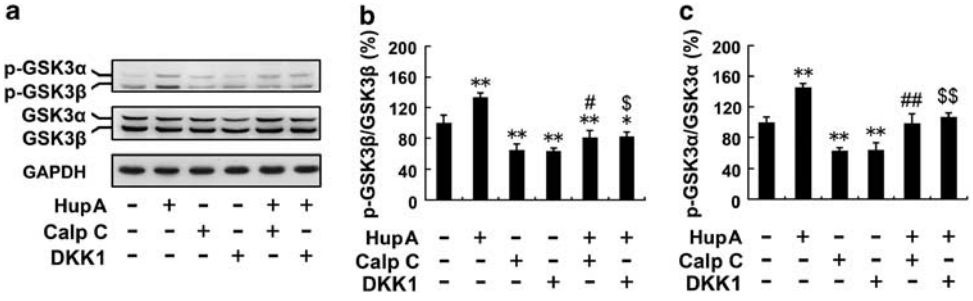

Figure 8 HupA inhibits the GSK3α/β activity in SH-SY5Y cells transfected with APPsw. (a) Immunoblots showing the levels of GSK3α/β and p-GSK3α/β in APPsw cells treated with HupA and inhibitors. GAPDH was used as an internal control. (b, c) HupA treatment significantly increased the ratio of p-GSK3β/GSK3β as well as p-GSK3α/GSK3α. Calphostin C or DKK1 treatment decreased the ratio of p-GSK3β/GSK3β and p-GSK3α/GSK3α, whereas HupA reversed the ratio of p-GSK3β/GSK3β and p-GSK3α/GSK3α in cultures pretreated with Calphostin C or DKK1 followed by HupA. The data shown in (b, c) are presented as the mean ± SEM of at least three independent experiments. $^{*}p < 0.05$, $^{**}p < 0.01$ *vs* control group; $^{\#}p < 0.05$, $^{\#\#}p < 0.01$ *vs* calphostin C-treated group; $^{\$}p < 0.05$, $^{\$\$}p < 0.01$ *vs* DKK1-treated group.

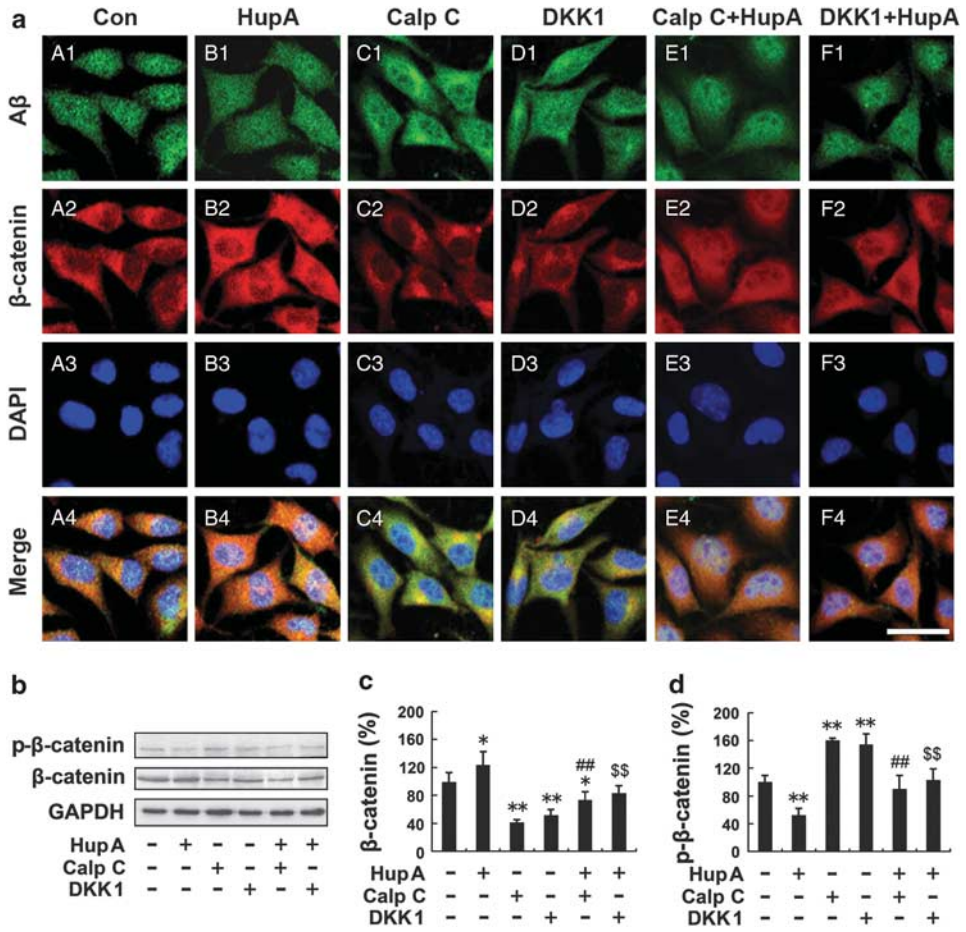

Figure 9 HupA increases the level of β-catenin in SH-SY5Y cells transfected with APPsw. (a) Double labeling of Aβ (A1–F1) and β-catenin (A2–F2) and confocal microscopic images showing the distribution and expression of β-catenin in APPsw cells. HupA treatment significantly increased the β-catenin immunofluorescence in APPsw cells (B2), compared with the control (A2). Calphostin C or DKK-1 treatment decreased the levels of β-catenin (C2 and D2). Additional HupA treatment reversed the reduction of β-catenin in cultures pretreated with inhibitors Calphostin C or DKK-1 (E2 and F2). Scale bar = 30 μm. (b) Western blot analysis showing the levels of β-catenin and p-β-catenin in APPsw cells treated with HupA or inhibitors. GAPDH was used as an internal control. (c, d) The protein level of total β-catenin was significantly increased, whereas the level of p-β-catenin was significantly decreased in HupA-treated cells compared with controls. There was a significantly reduced level of total β-catenin and an increased level of p-β-catenin in cultures treated with Calphostin C or DKK1, whereas the total β-catenin level was increased and the p-β-catenin level was reduced when cultures were preincubated with inhibitors followed by HupA. Representative immunoblots from three experiments are shown. The data shown in (c, d) are presented as mean ± SEM of at least three independent experiments. $^{**}p<0.05$, $^{**}p<0.01$ *vs* control group; $^{\#\#}p<0.01$ *vs* Calphostin C-treated group; $^{\$\$}p<0.01$ *vs* DKK1-treated group.

calphostin C and DKK-1 treatment reduced β-catenin immunofluorescence (Figure 9a, C2 and D2), whereas addition of HupA reversed the reduction of β-catenin in APPsw cells pretreated with inhibitors calphostin C and DKK-1 (Figure 9a, E2 and F2).

Immunoblotting results further confirmed the reversal effects of HupA on the changes in β-catenin in APPsw cells pretreated with inhibitors (Figure 9b). The protein levels of total β-catenin were significantly reduced by $40.92 \pm 4.46\%$ (calphostin C; $p<0.01$) and $51.05 \pm 8.84\%$ (DKK1; $p<0.01$) ($F(5, 24) = 18.382$, $p<0.05$; Figure 9c), whereas the levels of p-β-catenin were significantly increased by $159.85 \pm 3.70\%$ (calphostin C; $p<0.01$) and $153.86 \pm 15.49\%$ (DKK1; $p<0.01$) in cultures treated with inhibitors compared with controls ($F(5, 24) = 19.449$, $p<0.05$; Figure 9d). In cultures pretreated with inhibitors and then treated with HupA, the levels of β-catenin were reversed to $179.56 \pm 28.42\%$ (calphostin C + HupA) compared with the calphostin C-treated group ($p<0.01$), and $161.98 \pm 22.06\%$ (DKK1 + HupA) compared with the DKK1 treatment group ($p<0.01$; Figure 9c), and the levels of p-β-catenin were reversed to $56.02 \pm 12.41\%$ (calphostin C + HupA) compared with the calphostin C-treated group ($p<0.01$), and $66.87 \pm 10.39\%$ (DKK1 + HupA) compared with DKK1 treatment ($p<0.01$; Figure 9d). Taken together, these data further indicate that HupA reverses PKC- and Wnt-inhibitor-induced changes in Wnt/β-catenin signaling *in vitro*.

DISCUSSION

It has been previously reported that the intranasal administration of nasal gel containing HupA is a potential noninvasive strategy for the treatment of AD because it can provide similar plasma concentrations and high CSF concentrations of HupA compared with intravenous administration (Yue *et al*, 2007). In this study, involving treatment with nasal gel HupA in APP/PS1 transgenic mice, the effects

of HupA on the specific markers were confirmed, including inhibition of AChE, antioxidant activity, and enhancement of sAPPα release. Moreover, we showed for the first time that HupA upregulates β-catenin expression *in vivo* and *in vitro*, suggesting that the neuroprotective effect of HupA might be related to the regulation of the Wnt signaling pathway in the AD brain.

HupA is Involved in Regulation of the Wnt Signaling Pathway

It has been generally accepted that loss of Wnt signaling function is involved in Aβ-dependent neurodegeneration in the AD brain (Inestrosa and Toledo, 2008b). Studies have demonstrated that GSK3β and β-catenin, the two key components of the canonical Wnt signaling pathway, are altered dramatically in the AD model mouse brain (Zhang *et al*, 1998; Pei *et al*, 1999), and activation of Wnt signaling can prevent neurodegeneration induced by Aβ fibrils (De Ferrari *et al*, 2003). Interestingly, an *in vivo* study has shown that AChE–Aβ neurotoxicity is related to the changes in the expression levels of both GSK3β and β-catenin (Inestrosa *et al*, 2004). Importantly, a bifunctional (AChE inhibitor and anti-inflammatory) compound, IBU-PO, inhibits GSK3β and enhances β-catenin activity, preventing the loss of function of the Wnt signaling pathway caused by Aβ toxicity (Farias *et al*, 2005). These findings suggest that the neuroprotective effect of the AChE inhibitor is related to modulation of the Wnt/β-catenin signaling pathway (Inestrosa *et al*, 2008a; Toledo *et al*, 2008). In this study we showed that HupA, an AChE inhibitor, is involved in the regulation of Wnt signaling in APP/PS1 transgenic mouse and APPsw cell models. We present data showing that HupA significantly inhibits GSK3β activity and stabilizes the β-catenin protein level *in vivo* and *in vitro*, suggesting that activation of the Wnt signal transduction pathway is involved in the neuroprotective effects of HupA against Aβ neurotoxicity.

On the other hand, activation of both GSK3α and GSK3β through their autophosphorylation has been implicated in AD pathogenesis (Caricasole *et al*, 2004). Although there may be some crosslinking between GSK3α and GSK3β proteins, increased GSK3α activity is mainly involved in APP processing and Aβ generation (Phiel *et al*, 2003), whereas activation of GSK3β is predominantly associated with tau phosphorylation and neurofibrillary tangle formation (Baum *et al*, 1996; Ma *et al*, 2006). Several studies have shown that HupA has the ability to regulate APP processing *in vitro* (Zhang *et al*, 2004; Peng *et al*, 2007). We present data showing that there is a significant increase in the phosphorylation levels of both GSK3α and GSK3β proteins in HupA-treated APP/PS1 mouse brain and APPsw-overexpressing cells, suggesting that HupA can inhibit the activity of GSK3α/β and, hence, may inhibit Aβ generation and tau phosphorylation.

HupA Regulates the Processing of APP to the Nonamyloidogenic Pathway

Several lines of evidence indicate that through the α-secretase pathway, APP is cleaved within the sequence of the Aβ peptide and generates the sAPPα fragment (Esch *et al*, 1990), which is beneficial for neuronal survival (Mattson *et al*, 1997; Wallace *et al*, 1997), whereas through the β-secretase pathway, APP is cleaved to form neurotoxic Aβ and is involved in the pathogenesis of AD (Haass *et al*, 1992; Shoji *et al*, 1992; Bodles and Barger, 2005). Interestingly, the widely used AChE inhibitors, including donepezil, rivastigmine, and galantamine, have been shown to increase sAPPα release (Racchi *et al*, 2004). Recent studies have also shown that HupA can guide APP processing to the α-secretase pathway through mediating α-secretase activity and, hence, reduce Aβ generation in cultured cells (Zhang *et al*, 2004; Peng *et al*, 2007). In this study, we examined the effects of HupA on APP processing in the APP/PS1 mouse. Our data show that in the nasal gel HupA-treated transgenic mouse brain, the expression level of APP695 proteins is markedly reduced. HupA treatment significantly enhances the expression level of ADAM10, a candidate of α-secretase, and subsequently there is an increase in the levels of α-secretase-generated sAPPα and C83 fragments in transgenic mouse brain and in APPsw-transfected cells. Meanwhile, HupA reduces the levels of BACE1 and β-secretase-generated sAPPβ and C99 fragments *in vivo* and *in vitro*. Furthermore, in the HupA-treated APP/PS1 mouse brain, there is a reduction in Aβ levels and Aβ burden detected by ELISA and immunohistochemistry, respectively. Taken together, our results indicate that HupA modulates the processing of APP to the nonamyloidogenic pathway.

HupA Regulates APP Processing to the Nonamyloidogenic Pathway Through Activation of PKC and Wnt/β-Catenin Signaling

Crosstalk between PKC and Wnt/β-catenin signaling is involved in the modulation of GSK3 activation. Several studies have shown that activation of PKC inhibits the activity of GSK-3β and modulates Wnt/β-catenin signaling (Chen *et al*, 2000; Garrido *et al*, 2002). On the other hand, activation of Wnt/β-catenin signaling prevents neuronal apoptosis in a PKC-dependent manner (Chen *et al*, 2000; De Ferrari *et al*, 2003; Alvarez *et al*, 2004). Although the mechanism of GSK3 modulation in the AD brain is far from fully understood, the involvement of both Wnt signaling and PKC in the abnormal activation of GSK3 has caused increasing concern. A recent study has shown that HupA may affect the processing of APP by upregulation of PKC (Zhang *et al*, 2004). In our *in vitro* studies, we found that HupA reverses PKC- and Wnt-inhibitor-induced inhibition of nonamyloidogenic processing of APP, paralleled by an inactivation of GSK3 and a reversal of the level of β-catenin. As GSK3 is involved in APP processing (Phiel *et al*, 2003) and tau phosphorylation (Baum *et al*, 1996), it is reasonable to speculate that the HupA regulation of APP processing to the nonamyloidogenic pathway is, at least partly, through activation of PKC and Wnt/β-catenin signaling.

Intranasal Administration of HupA May Be a Reasonable Approach to AD Treatment

Drug delivery to the brain via the nasal route is a subject of increasing interest because the nasal mucosa offers rapid absorption with an abundantly vascularized and relatively large absorptive surface area (Turker *et al*, 2004), does not

require a complicated administration method, and can easily be carried out by medical services for chronic care such as in the case of AD. For the AChE inhibitors, it has been reported that nasal administration of galantamine can enhance the bioavailability and reduce the emetic response (Leonard *et al*, 2007). Nasal gel HupA can provide similar plasma concentrations after 15 min and higher CSF concentrations after 30 min than those following intravenous administration (Yue *et al*, 2007). In this study, intranasal administration of nasal gel HupA exhibits AChE inhibition and antioxidative effects on APP/PS1 mouse brain, which have been confirmed before by traditional administration methods, such as intravenous and oral administration (Wang *et al*, 2000; Wang *et al*, 2001; Wang *et al*, 2006b). Our data also show that HupA regulates the processing of APP to the nonamyloidogenic pathway. In addition, we confirmed the safety of nasal gel HupA administration by examining the structure of the mucosal cilia. We also assessed if long-term intranasal administration of HupA might influence the structure of the olfactory bulb. Our data showed that intranasal administration of HupA did not significantly alter the structure and the expression levels of OMP and GAP-43 in the olfactory bulb. Furthermore, nasal gel HupA treatment did not alter the neurogenesis in the SVZ of APP/PS1 mouse brain. Although we did not find BrdU-labeled cells in the bulb, the similar distribution of BrdU-positive cells in the SVZ in the vehicle- and nasal gel HupA-treated mouse brain indicates that the newborn cells in the SVZ migrate to the bulb through the rostral migratory stream, which might not be affected by the administration of HupA. Moreover, the result of EB leakage assay in our study demonstrated that nasal gel HupA treatment did not induce significant alterations of BBB in the transgenic mouse brain. The present data, together with previous studies (Yue *et al*, 2007), suggest that intranasal administration of nasal gel HupA may represent a safe and noninvasive therapeutic strategy for the treatment of AD.

ACKNOWLEDGEMENTS

The study was supported by the Natural Science Foundation of China (30770680), the Program for New Century Excellent Talents in University (NCET-04-0288), the China Postdoctoral Science Foundation (2005037008), the Specialized Research Fund for the Doctoral Program of Higher Education (SRFDP-20060159001), and the National Basic Research Program of China (973 Program 2009CB930300).

DISCLOSURE

The authors declare no conflict of interest.

REFERENCES

Akaike A, Takada-Takatori Y, Kume T, Izumi Y (2010). Mechanisms of neuroprotective effects of nicotine and acetylcholinesterase inhibitors: role of alpha4 and alpha7 receptors in neuroprotection. *J Mol Neurosci* **40**: 211–216.

Alisky JM (2006). Cholinesterase inhibitors might alleviate methamphetamine-induced delusions, hallucinations and cognitive impairment, while reducing craving and addiction. *World J Biol Psychiatry* **7**: 269.

Alvarez A, Alarcon R, Opazo C, Campos EO, Munoz FJ, Calderon FH *et al* (1998). Stable complexes involving acetylcholinesterase and amyloid-beta peptide change the biochemical properties of the enzyme and increase the neurotoxicity of Alzheimer's fibrils. *J Neurosci* **18**: 3213–3223.

Alvarez A, Opazo C, Alarcon R, Garrido J, Inestrosa NC (1997). Acetylcholinesterase promotes the aggregation of amyloid-beta-peptide fragments by forming a complex with the growing fibrils. *J Mol Biol* **272**: 348–361.

Alvarez AR, Godoy JA, Mullendorff K, Olivares GH, Bronfman M, Inestrosa NC (2004). Wnt-3a overcomes beta-amyloid toxicity in rat hippocampal neurons. *Exp Cell Res* **297**: 186–196.

Alvarez G, Munoz-Montano JR, Satrustegui J, Avila J, Bogonez E, Diaz-Nido J (1999). Lithium protects cultured neurons against beta-amyloid-induced neurodegeneration. *FEBS Lett* **453**: 260–264.

Baum L, Hansen L, Masliah E, Saitoh T (1996). Glycogen synthase kinase 3 alteration in Alzheimer disease is related to neurofibrillary tangle formation. *Mol Chem Neuropathol* **29**: 253–261.

Bodles AM, Barger SW (2005). Secreted beta-amyloid precursor protein activates microglia via JNK and p38-MAPK. *Neurobiol Aging* **26**: 9–16.

Caricasole A, Copani A, Caraci F, Aronica E, Rozemuller AJ, Caruso A *et al* (2004). Induction of Dickkopf-1, a negative modulator of the Wnt pathway, is associated with neuronal degeneration in Alzheimer's brain. *J Neurosci* **24**: 6021–6027.

Ceravolo R, Volterrani D, Tognoni G, Dell'Agnello G, Manca G, Kiferle L *et al* (2004). Cerebral perfusional effects of cholinesterase inhibitors in Alzheimer disease. *Clin Neuropharmacol* **27**: 166–170.

Chen RH, Ding WV, McCormick F (2000). Wnt signaling to beta-catenin involves two interactive components. Glycogen synthase kinase-3beta inhibition and activation of protein kinase C. *J Biol Chem* **275**: 17894–17899.

Cheng DH, Ren H, Tang XC (1996). Huperzine A, a novel promising acetylcholinesterase inhibitor. *NeuroReport* **8**: 97–101.

Cheng DH, Tang XC (1998). Comparative studies of huperzine A, E2020, and tacrine on behavior and cholinesterase activities. *Pharmacol Biochem Behav* **60**: 377–386.

Cook D, Fry MJ, Hughes K, Sumathipala R, Woodgett JR, Dale TC (1996). Wingless inactivates glycogen synthase kinase-3 via an intracellular signalling pathway which involves a protein kinase C. *EMBO J* **15**: 4526–4536.

De Ferrari GV, Chacon MA, Barria MI, Garrido JL, Godoy JA, Olivares G *et al* (2003). Activation of Wnt signaling rescues neurodegeneration and behavioral impairments induced by beta-amyloid fibrils. *Mol Psychiatry* **8**: 195–208.

Erkinjuntti T, Roman G, Gauthier S (2004). Treatment of vascular dementia—evidence from clinical trials with cholinesterase inhibitors. *J Neurol Sci* **226**: 63–66.

Esch FS, Keim PS, Beattie EC, Blacher RW, Culwell AR, Oltersdorf T *et al* (1990). Cleavage of amyloid beta peptide during constitutive processing of its precursor. *Science* **248**: 1122–1124.

Farias GG, Godoy JA, Vazquez MC, Adani R, Meshulam H, Avila J *et al* (2005). The anti-inflammatory and cholinesterase inhibitor bifunctional compound IBU-PO protects from beta-amyloid neurotoxicity by acting on Wnt signaling components. *Neurobiol Dis* **18**: 176–183.

Garrido JL, Godoy JA, Alvarez A, Bronfman M, Inestrosa NC (2002). Protein kinase C inhibits amyloid beta peptide neurotoxicity by acting on members of the Wnt pathway. *FASEB J* **16**: 1982–1984.

Geula C, Mesulam MM (1995). Cholinesterases and the pathology of Alzheimer disease. *Alzheimer Dis Assoc Disord* **9**(Suppl 2): 23–28.

Guillozet AL, Smiley JF, Mash DC, Mesulam MM (1997). Butyrylcholinesterase in the life cycle of amyloid plaques. *Ann Neurol* **42**: 909–918.

Haass C, Schlossmacher MG, Hung AY, Vigo-Pelfrey C, Mellon A, Ostaszewski BL *et al* (1992). Amyloid beta-peptide is produced by cultured cells during normal metabolism. *Nature* **359**: 322–325.

Holick KA, Lee DC, Hen R, Dulawa SC (2008). Behavioral effects of chronic fluoxetine in BALB/cJ mice do not require adult hippocampal neurogenesis or the serotonin 1A receptor. *Neuropsychopharmacology* **33**: 406–417.

Inestrosa NC, Alvarez A, Dinamarca MC, Perez-Acle T, Colombres M (2005). Acetylcholinesterase-amyloid-beta-peptide interaction: effect of Congo Red and the role of the Wnt pathway. *Curr Alzheimer Res* **2**: 301–306.

Inestrosa NC, Alvarez A, Godoy J, Reyes A, De Ferrari GV (2000). Acetylcholinesterase-amyloid-beta-peptide interaction and Wnt signaling involvement in Abeta neurotoxicity. *Acta Neurol Scand Suppl* **176**: 53–59.

Inestrosa NC, Dinamarca MC, Alvarez A (2008a). Amyloid-cholinesterase interactions. Implications for Alzheimer's disease. *FEBS J* **275**: 625–632.

Inestrosa NC, Toledo EM (2008b). The role of Wnt signaling in neuronal dysfunction in Alzheimer's disease. *Mol Neurodegener* **3**: 9.

Inestrosa NC, Urra S, Colombres M (2004). Acetylcholinesterase (AChE)–amyloid-beta-peptide complexes in Alzheimer's disease. The Wnt signaling pathway. *Curr Alzheimer Res* **1**: 249–254.

Kim WR, Kim Y, Eun B, Park OH, Kim H, Kim K *et al* (2007). Impaired migration in the rostral migratory stream but spared olfactory function after the elimination of programmed cell death in Bax knock-out mice. *J Neurosci* **27**: 14392–14403.

Kuhn HG, Dickinson-Anson H, Gage FH (1996). Neurogenesis in the dentate gyrus of the adult rat: age-related decrease of neuronal progenitor proliferation. *J Neurosci* **16**: 2027–2033.

Lahiri DK, Rogers JT, Greig NH, Sambamurti K (2004). Rationale for the development of cholinesterase inhibitors as anti-Alzheimer agents. *Curr Pharm Des* **10**: 3111–3119.

Lahoud-Rahme MS, Stezoski J, Kochanek PM, Melick J, Tisherman SA, Drabek T (2009). Blood-brain barrier integrity in a rat model of emergency preservation and resuscitation. *Resuscitation* **80**: 484–488.

Lenzser G, Kis B, Snipes JA, Gaspar T, Sandor P, Komjati K *et al* (2007). Contribution of poly(ADP-ribose) polymerase to post-ischemic blood-brain barrier damage in rats. *J Cereb Blood Flow Metab* **27**: 1318–1326.

Leonard AK, Sileno AP, Brandt GC, Foerder CA, Quay SC, Costantino HR (2007). In vitro formulation optimization of intranasal galantamine leading to enhanced bioavailability and reduced emetic response in vivo. *Int J Pharm* **335**: 138–146.

Ma QL, Lim GP, Harris-White ME, Yang F, Ambegaokar SS, Ubeda OJ *et al* (2006). Antibodies against beta-amyloid reduce Abeta oligomers, glycogen synthase kinase-3beta activation and tau phosphorylation in vivo and in vitro. *J Neurosci Res* **83**: 374–384.

Marks DR, Tucker K, Cavallin MA, Mast TG, Fadool DA (2009). Awake intranasal insulin delivery modifies protein complexes and alters memory, anxiety, and olfactory behaviors. *J Neurosci* **29**: 6734–6751.

Mattson MP, Barger SW, Furukawa K, Bruce AJ, Wyss-Coray T, Mark RJ *et al* (1997). Cellular signaling roles of TGF beta, TNF alpha and beta APP in brain injury responses and Alzheimer's disease. *Brain Res Brain Res Rev* **23**: 47–61.

Moon RT, Bowerman B, Boutros M, Perrimon N (2002). The promise and perils of Wnt signaling through beta-catenin. *Science* **296**: 1644–1646.

Mori E, Hashimoto M, Krishnan KR, Doraiswamy PM (2006). What constitutes clinical evidence for neuroprotection in Alzheimer disease: support for the cholinesterase inhibitors? *Alzheimer Dis Assoc Disord* **20**(2 Suppl 1): S 19–S 26.

Munoz FJ, Inestrosa NC (1999). Neurotoxicity of acetylcholinesterase amyloid beta-peptide aggregates is dependent on the type of Abeta peptide and the AChE concentration present in the complexes. *FEBS Lett* **450**: 205–209.

Muyllaert D, Terwel D, Borghgraef P, Devijver H, Dewachter I, Van Leuven F (2006). Transgenic mouse models for Alzheimer's disease: the role of GSK-3B in combined amyloid and tau-pathology. *Rev Neurol (Paris)* **162**: 903–907.

Patapoutian A, Reichardt LF (2000). Roles of Wnt proteins in neural development and maintenance. *Curr Opin Neurobiol* **10**: 392–399.

Pei JJ, Braak E, Braak H, Grundke-Iqbal I, Iqbal K, Winblad B *et al* (1999). Distribution of active glycogen synthase kinase 3beta (GSK-3beta) in brains staged for Alzheimer disease neurofibrillary changes. *J Neuropathol Exp Neurol* **58**: 1010–1019.

Peng Y, Jiang L, Lee DY, Schachter SC, Ma Z, Lemere CA (2006). Effects of huperzine A on amyloid precursor protein processing and beta-amyloid generation in human embryonic kidney 293 APP Swedish mutant cells. *J Neurosci Res* **84**: 903–911.

Peng Y, Lee DY, Jiang L, Ma Z, Schachter SC, Lemere CA (2007). Huperzine A regulates amyloid precursor protein processing via protein kinase C and mitogen-activated protein kinase pathways in neuroblastoma SK-N-SH cells over-expressing wild type human amyloid precursor protein 695. *Neuroscience* **150**: 386–395.

Phiel CJ, Wilson CA, Lee VM, Klein PS (2003). GSK-3alpha regulates production of Alzheimer's disease amyloid-beta peptides. *Nature* **423**: 435–439.

Racchi M, Mazzucchelli M, Porrello E, Lanni C, Govoni S (2004). Acetylcholinesterase inhibitors: novel activities of old molecules. *Pharmacol Res* **50**: 441–451.

Reyes AE, Chacon MA, Dinamarca MC, Cerpa W, Morgan C, Inestrosa NC (2004). Acetylcholinesterase-Abeta complexes are more toxic than Abeta fibrils in rat hippocampus: effect on rat beta-amyloid aggregation, laminin expression, reactive astrocytosis, and neuronal cell loss. *Am J Pathol* **164**: 2163–2174.

Rochefort C, Gheusi G, Vincent JD, Lledo PM (2002). Enriched odor exposure increases the number of newborn neurons in the adult olfactory bulb and improves odor memory. *J Neurosci* **22**: 2679–2689.

Sheldahl LC, Park M, Malbon CC, Moon RT (1999). Protein kinase C is differentially stimulated by Wnt and Frizzled homologs in a G-protein-dependent manner. *Curr Biol* **9**: 695–698.

Shoji M, Golde TE, Ghiso J, Cheung TT, Estus S, Shaffer LM *et al* (1992). Production of the Alzheimer amyloid beta protein by normal proteolytic processing. *Science* **258**: 126–129.

Sicras A, Rejas-Gutierrez J (2004). Drug-cholinesterase-inhibitors persistence patterns in treated patients with dementia of Alzheimer type: retrospective comparative analysis of donepezil, rivastigmine and galantamine. *Rev Neurol* **39**: 312–316.

Tang LL, Wang R, Tang XC (2005). Huperzine A protects SHSY5Y neuroblastoma cells against oxidative stress damage via nerve growth factor production. *Eur J Pharmacol* **519**: 9–15.

Tang W, Zhang Y, Gao J, Ding X, Gao S (2008). The anti-fatigue effect of 20(R)-ginsenoside Rg3 in mice by intranasally administration. *Biol Pharm Bull* **31**: 2024–2027.

Toledo EM, Colombres M, Inestrosa NC (2008). Wnt signaling in neuroprotection and stem cell differentiation. *Prog Neurobiol* **86**: 281–296.

Turker S, Onur E, Ozer Y (2004). Nasal route and drug delivery systems. *Pharm World Sci* **26**: 137–142.

van der Staay FJ, Bouger PC (2005). Effects of the cholinesterase inhibitors donepezil and metrifonate on scopolamine-induced impairments in the spatial cone field orientation task in rats. *Behav Brain Res* **156**: 1–10.

Ved HS, Koenig ML, Dave JR, Doctor BP (1997). Huperzine A, a potential therapeutic agent for dementia, reduces neuronal cell death caused by glutamate. *NeuroReport* **8**: 963–968.

Wallace WC, Akar CA, Lyons WE (1997). Amyloid precursor protein potentiates the neurotrophic activity of NGF. *Brain Res Mol Brain Res* **52**: 201–212.

Wang LM, Han YF, Tang XC (2000). Huperzine A improves cognitive deficits caused by chronic cerebral hypoperfusion in rats. *Eur J Pharmacol* **398**: 65–72.

Wang R, Yan H, Tang XC (2006a). Progress in studies of huperzine A, a natural cholinesterase inhibitor from Chinese herbal medicine. *Acta Pharmacol Sin* **27**: 1–26.

Wang R, Zhang HY, Tang XC (2001). Huperzine A attenuates cognitive dysfunction and neuronal degeneration caused by beta-amyloid protein-(1–40) in rat. *Eur J Pharmacol* **421**: 149–156.

Wang ZF, Tang LL, Yan H, Wang YJ, Tang XC (2006b). Effects of huperzine A on memory deficits and neurotrophic factors production after transient cerebral ischemia and reperfusion in mice. *Pharmacol Biochem Behav* **83**: 603–611.

Wang ZF, Tang XC (2007). Huperzine A protects C6 rat glioma cells against oxygen-glucose deprivation-induced injury. *FEBS Lett* **581**: 596–602.

Wang ZF, Wang J, Zhang HY, Tang XC (2008). Huperzine A exhibits anti-inflammatory and neuroprotective effects in a rat model of transient focal cerebral ischemia. *J Neurochem* **106**: 1594–1603.

Willert K, Nusse R (1998). Beta-catenin: a key mediator of Wnt signaling. *Curr Opin Genet Dev* **8**: 95–102.

Yagi N, Taniuchi Y, Hamada K, Sudo J, Sekikawa H (2002). Pharmacokinetics of ketotifen fumarate after intravenous, intranasal, oral and rectal administration in rabbits. *Biol Pharm Bull* **25**: 1614–1618.

Yan H, Zhang HY, Tang XC (2007). Involvement of M1-muscarinic acetylcholine receptors, protein kinase C and mitogen-activated protein kinase in the effect of huperzine A on secretory amyloid precursor protein-alpha. *NeuroReport* **18**: 689–692.

Yu S, Zheng W, Xin N, Chi ZH, Wang NQ, Nie YX *et al* (2010). Curcumin prevents dopaminergic neuronal death through inhibition of the c-Jun N-terminal kinase pathway. *Rejuvenation Res* **13**: 55–64.

Yue P, Tao T, Zhao Y, Ren J, Chai X (2007). Huperzine A in rat plasma and CSF following intranasal administration. *Int J Pharm* **337**: 127–132.

Zhang HY, Tang XC (2006). Neuroprotective effects of huperzine A: new therapeutic targets for neurodegenerative disease. *Trends Pharmacol Sci* **27**: 619–625.

Zhang HY, Yan H, Tang XC (2004). Huperzine A enhances the level of secretory amyloid precursor protein and protein kinase C-alpha in intracerebroventricular beta-amyloid-(1–40) infused rats and human embryonic kidney 293 Swedish mutant cells. *Neurosci Lett* **360**: 21–24.

Zhang HY, Yan H, Tang XC (2008a). Non-cholinergic effects of huperzine A: beyond inhibition of acetylcholinesterase. *Cell Mol Neurobiol* **28**: 173–183.

Zhang HY, Zheng CY, Yan H, Wang ZF, Tang LL, Gao X *et al* (2008b). Potential therapeutic targets of huperzine A for Alzheimer's disease and vascular dementia. *Chem Biol Interact* **175**: 396–402.

Zhang J, Liu Q, Chen Q, Liu NQ, Li FL, Lu ZB *et al* (2006a). Nicotine attenuates beta-amyloid-induced neurotoxicity by regulating metal homeostasis. *FASEB J* **20**: 1212–1214.

Zhang J, Mori A, Chen Q, Zhao B (2006b). Fermented papaya preparation attenuates beta-amyloid precursor protein: beta-amyloid-mediated copper neurotoxicity in beta-amyloid precursor protein and beta-amyloid precursor protein Swedish mutation overexpressing SH-SY5Y cells. *Neuroscience* **143**: 63–72.

Zhang Z, Hartmann H, Do VM, Abramowski D, Sturchler-Pierrat C, Staufenbiel M *et al* (1998). Destabilization of beta-catenin by mutations in presenilin-1 potentiates neuronal apoptosis. *Nature* **395**: 698–702.

Zheng W, Xin N, Chi ZH, Zhao BL, Zhang J, Li JY *et al* (2009). Divalent metal transporter 1 is involved in amyloid precursor protein processing and Abeta generation. *FASEB J* **23**: 4207–4217.

Zhu XD, Giacobini E (1995). Second generation cholinesterase inhibitors: effect of (L)-huperzine-A on cortical biogenic amines. *J Neurosci Res* **41**: 828–835.